



Recent Advances in the Synthesis of Electron Donor Conjugated Terpolymers for Solar Cell Applications

Desta Gedefaw^{1*}, Xun Pan² and Mats R. Andersson^{2*}

¹ School of Biological and Chemical Sciences, The University of the South Pacific, Suva, Fiji, ² Flinders Institute for Nanoscale Science and Technology, Flinders University, Bedford Park, Adelaide, SA, Australia

OPEN ACCESS

Edited by:

Dong Wook Chang,
Pukyong National University,
South Korea

Reviewed by:

Ping Deng,
Fuzhou University, China
Jialiang Wang,
University of Wisconsin-Madison,
United States

*Correspondence:

Desta Gedefaw
gedefaw_d@usp.ac.fj
Mats R. Andersson
mats.andersson@flinders.edu.au

Specialty section:

This article was submitted to
Energy Materials,
a section of the journal
Frontiers in Materials

Received: 29 May 2020

Accepted: 27 July 2020

Published: 18 August 2020

Citation:

Gedefaw D, Pan X and
Andersson MR (2020) Recent
Advances in the Synthesis of Electron
Donor Conjugated Terpolymers
for Solar Cell Applications.
Front. Mater. 7:280.
doi: 10.3389/fmats.2020.00280

The synthesis of donor (D)-acceptor (A) polymers using structurally elaborated monomers is an active research field. Some of the challenges with the use of alternating D-A polymers for photovoltaic applications are the relatively narrow absorption widths, the presence of absorption valleys in the visible region, unoptimized molecular energy levels and even lack of compatibility of the polymers with the common acceptors. The synthesis and characterization of polymers consisting of multiple chromophores (random and regular terpolymers) with complementing properties is currently gaining momentum in order to delicately optimize properties of polymers. A random terpolymer can either be of a system composed of one donor and two acceptors [(D-A1)-ran-(D-A2)] or a one acceptor and two donor segments [(D1-A)-ran-(D2-A)] incorporated in the polymer backbone. By varying the composition of the monomers in the feed of the polymerization reaction, the properties of the resulting terpolymers can be carefully optimized. Using this strategy, many materials with desired properties have been developed and power conversion efficiency (PCE) surpassing 14% in a single layer bulk heterojunction (BHJ) solar cell device have been reported. This review summarizes the most recent advances made in the development of electron donor terpolymers for organic photovoltaics (OPVs). The properties of the terpolymers are compared with their respective reference polymer.

Keywords: conjugated polymers, solar cells, terpolymers, random terpolymers, regular terpolymers

INTRODUCTION

Conjugated polymers and small molecules have been the focus of research in the past few decades because of the clear advantage they potentially offer in the production of cheap products in various fields such as organic field-effect transistors (OFETs), organic photovoltaics (OPVs) and light-emitting diodes (LEDs). In OPVs, the photoactive material commonly consists of a blend of electron rich polymer (donor) and electron deficient (acceptor) materials intermixed on a nanometer scale. Among the various donor polymer architectures, polymers consisting of single molecular repeating units (homopolymers) were of interest in OPV research community. Repeating units such as thiophenes and benzodithiophenes have been utilized for the synthesis of the corresponding homopolymers with necessary modifications introduced to the core aromatic molecular units to

impart desired properties such as good solubility, desired level of crystallinity, high optical coverage and desired molecular energy levels on the resulting polymers (Elsenbaumer et al., 1986; Almeida et al., 2009; Lee et al., 2012; Cai et al., 2017). Even though there have been tremendous progresses in the synthetic methodology for the structural modifications of the monomers, there are still inherent shortcomings of homopolymers such as narrow absorption band and mostly raised HOMO energy levels and hence yielding a relatively lower photovoltaic performances. In order to circumvent the narrow absorption profile and modulate the molecular energy levels, a “the Donor-Acceptor (D-A) design motif” where an electron rich (donor) and electron deficient (acceptor) aromatic fragments are linked together by a covalent bond was developed (Havinga et al., 1992; Gedefaw et al., 2017a; Gedefaw and Andersson, 2019; Atli et al., 2020).

The D-A strategy have enabled synthetic chemists to better control the optoelectronic properties of conjugated polymers and small molecules to produce materials (Kitamura et al., 1996; Cheng et al., 2009).

Along with the synthesis of novel conjugated materials with desired properties, significant advances have been achieved in device structures and optimization techniques (Glenis et al., 1984; Tang, 1986; Halls et al., 1995; Yu et al., 1995; Granström et al., 1998; Johannes et al., 2004). With the continued enhanced understanding of the nature of film microstructure (Bolognesi et al., 2016) and meticulous device optimization efforts (Li et al., 2014), PCE in the range of 14–18% with a binary blend and tandem OPVs have been reported (Li S. et al., 2018; Meng et al., 2018; Zhang et al., 2018; Chen, 2019; Cui et al., 2019; Fan et al., 2019; Xu et al., 2019b; Liu Q. et al., 2020; Luo et al., 2020; Salim et al., 2020). One of the promising feature of organic solar cells is the solution processability of the photoactive materials, which have opened the possibility of fabrication of photovoltaic devices using printing technologies at a relatively lower cost (Hoth et al., 2007; Aernouts et al., 2008; Sumaiya et al., 2017).

The synthesis of well-defined polymers with pre-determined composition and structure is vital in order to have a control in the properties of conjugated polymers. Many of the monomeric units developed in the past have highly elaborated molecular features. Besides the challenges encountered in the synthesis of these monomers, the final polymers end up to have a narrow absorption profile, unoptimized energy levels and poor compatibility with the acceptor counterparts, resulting in a material that will likely perform less efficiently in organic solar cells. One way to tune the optical and electrochemical properties of polymers is by incorporating multiple chromophores such as three monomeric units in the polymer chains. According to IUPAC definition, polymers consisting more than one species of monomers (real, implicit or hypothetical) are called co-polymers (Jenkins et al., 1996). The polymers discussed in this paper consists of two species of monomers and not three different species of monomers as in terpolymers. Interestingly, this type of polymers are normally referred to as terpolymers in the literature and therefore we also call them terpolymers in the article (Jenkins et al., 1996). Recently, the synthesis and use of terpolymers for photovoltaics have gained tremendous attention (Colella et al., 2011; Khlyabich et al., 2011; Paulsen et al., 2014; Scott et al., 2019;

Gao et al., 2020). Terpolymers can either be random or regular. In random terpolymers, two acceptors and one donor monomers (D, A1, and A2) or two donors and one acceptor (A, D1, and D2) in a predetermined feed ratio of the monomers are introduced for the polymerization reaction, where the monomeric units will be assembled in the backbone of the polymer randomly to yield a polymer structure of the type (D-A1)-*ran*-(D-A2) or (A-D1)-*ran*-(A-D2), respectively. In regular terpolymers on the other hand, a properly functionalized D1-A-D2 or A1-D-A2 based monomeric segments are reacted with a functionalized acceptor (A) or donor (D), respectively, to form an alternating polymer. The diversity of monomers developed in the past allows the synthesis of countless multi-component materials with tailored properties (Heintges et al., 2020). The regular terpolymers have definite composition and hence provides the possibility of better control of the electronic properties (Heintges et al., 2020). It is expected that regular terpolymers to display a better inter polymer chain interaction due to the defined monomeric composition in the chain and hence are expected to have higher crystallinity. For instance, Heo et al. have demonstrated that a regioregular polymer prepared based on dithieno[3,2-b:2',3'-d]silole (DTS, D1), benzo[1,2-b:4,5-b]dithiophene (BDT, D2), and thieno[3,4-b]thiophene (TT, A) monomeric units to have a higher crystallinity and displayed a stronger absorption coefficient. Due to these advantages possessed, the regioregular polymer performed well in photovoltaic devices (Heo et al., 2016; Heintges et al., 2020). On the other hand, random terpolymers have less defined composition of the monomeric segments in the final polymer structure. Though the composition of the monomers in the feed is precisely known, the composition of the monomeric segments in the resulting polymer could either be same as the feed or it could be different depending on the polymerization kinetics of the monomers. In the same work as above, the random terpolymer prepared from DTS, BDT and TT showed a broadening toward higher wavelengths in the optical study ascribed to -TT-DTS-TT-DTS enriched segments. This is an interesting example that demonstrates how the polymerization kinetics affect the optical property and also how tricky predicting properties of random terpolymers will be unless the reactivity of the monomers are known (Heo et al., 2016).

Though random terpolymers have undefined composition, several of them have shown promising performances, which heralds the great potential of the strategy to produce tailored and efficient polymer donors and non-fullerene acceptors (Pan et al., 2017; Song et al., 2018; Wang et al., 2019, 2020; Yang et al., 2019; Zhang et al., 2020). Random terpolymers are also hailed from the point of view of reducing material cost by using a cheaper third component without compromising the efficiency (Jiang et al., 2016). These promising classes of terpolymers have been reviewed in the past. Some of the reported articles have attempted to classify the polymers based on the material properties such as complimentary absorption, crystallinity, morphology and so on (Luo et al., 2018; Gao et al., 2020). Herein, terpolymers (regular and random) developed recently are discussed in the following approach. The materials were first classified in two broad groups: polymers having two donors and two acceptors. Then, the polymers further grouped based on the type of acceptor

used to construct the terpolymers. The properties of terpolymers are then thoroughly discussed in terms of the optical properties, morphology, and crystallinity and so on. The properties of the terpolymers were compared with reference alternating polymers.

TERPOLYMERS CONSISTING TWO DONORS AND ONE ACCEPTOR UNITS

Here, terpolymers prepared from two electron rich and an electron deficient monomers are discussed. The optical, electrochemical and photovoltaic properties of the terpolymers are compared with the reference polymers. The terpolymers are classified based on the acceptor type.

Diketopyrrolopyrrole (DPP) and Other Lactam Ring Based Polymers

Among the various electron deficient molecular units developed to date, the DPP lactam ring is widely known in OPV research and has been incorporated in many D-A polymers (Hendriks et al., 2013; Choi et al., 2015; Zheng et al., 2016). In order to exploit the peculiar properties of random terpolymers in tuning physico-chemical properties, Ko et al. (2015) reported regular (**P1** Reg-PBDPPT) and random (**P2** Ran-PBDPPT) terpolymers based on (E)-1,2-di(thiophen-2-yl)ethene, 2,2'-bithiophene and DPP monomers (**Figure 1**). The two terpolymers (**P1** and **P2**) showed comparable optical and electrochemical properties (**Table 1**). The properties of the reference alternating polymers synthesized (**P3** PDPPBT and **P4** PDPPTVT) are also tabulated in **Table 1**. A blend of **P1** or **P2** with PC₇₁BM, processed from a chloroform: *o*-dichlorobenzene (ODCB) (4:1 v/v) solvent, was embedded between PEDOT:PSS and Li/Al electrodes to investigate the photovoltaic properties. The regular terpolymer (**P1**) based optimized photovoltaic device gave a PCE of 5.45% while the random terpolymer (**P2**) based device gave a 5.24% PCE with 2% diiodooctane (DIO) solvent additive. The slightly higher PCE of the devices based on the regular terpolymer (**P1**) is mainly due to the higher fill factor (FF) achieved due to well-formed nanophase crystalline domains as observed with atomic force microscopy (AFM) and transmission electron microscopy (TEM) images. **P1** based devices gave a FF = 71% compared to a FF = 65% from **P2** based devices. The photovoltaic performance of **P3** and **P4** (reference polymers) were also studied with and without the DIO solvent additive. A 1:2 wt/wt blend of each of the polymers (**P3**) and (**P4**) with PC₇₁BM as a photoactive material processed from chloroform and ODCB (4:1 v/v) with DIO additive achieved a maximum PCE of 4.66 and 3.84%, respectively. In contrast to the devices prepared from the terpolymers, the reference D-A polymers (**P3** and **P4**) based devices showed a much coarser surface textures and microphase segregation in the internal structure as studied by AFM and scanning electron microscopy (SEM), which is the cause for the lower short circuit current (J_{SC}) and lower PCE of the devices (**Table 1**).

The effect of aromatic π -linkers in the properties of many D-A type polymers were studied in the past. For instance, thieno[3,2-b]thiophene as a π -linker of quinoxaline and BDT

based monomer have resulted in an alternating polymer with a rigid, planar and linear backbone structure compared to the use of thiophene as π -linker (Gedefaw et al., 2014). A systematic study on the effect of aromatic π -linkers in random terpolymers were studied in DPP based polymers. The DPP base monomer was copolymerized with quaterthiophene (QT) donor unit with the random introduction of various aromatic monomers as a third component. Consequently, random terpolymers denoted as **P5** P4TFDPP, **P6** P4TPDPP, **P7** P5TDPP, and **P8** P4TVDDPP consisting of fluorene, phenyl, thiophene and vinyl units as third components, respectively, were reported. **P7** and **P8** were synthesized by Stille metal catalyzed cross coupling reaction while **P5** and **P6** were prepared by Suzuki cross coupling reactions, using the properly functionalized monomeric units and reaction conditions in both systems (**Figure 1**; SambathKumar et al., 2016). The structure-property relationships of the polymers was investigated with DFT on optimized geometry consisting of two repeating units. Hence, the dihedral angles measured between thiophene and the linker unit (fluorene, phenyl, thiophene, and vinyl) vary between 19° and 25° for **P5** and **P6** dimers compared to a lower dihedral angle in the range of 1° and 10° for **P7** and **P8** dimers. The large dihedral angle for **P5** and **P6** is presumed to be due the bulky nature of fluorene and benzene aromatic linkers resulting in a twisted backbone. As expected, **P8** and **P7** with thiophene and vinyl linkers, respectively, gave a red shifted absorption with an onset of optical absorption in thin film reaching above 1000 nm. The vinyl linker is particularly known at promoting intermolecular π - π stacking, extending conjugation length and shifting of absorption to a longer wavelength (Chen et al., 2012). However, a blue shifted optical absorption of the polymers with benzene and fluorene π -linkers (**P5** and **P6**) were found likely due to the twisted nature of the polymer backbones. The HOMO and LUMO energy levels of the polymers were estimated using cyclic voltammetry (CV). Consistent with the optically determined band gap, **P8** showed a narrow band gap (1.22 eV) from the CV measurement due to the raised HOMO and lowered LUMO energy levels. The fluorene linked polymer (**P5**) showed the deepest HOMO (-5.46 eV) energy level compared to the other three polymers, which is vital to generate a higher open circuit voltage (V_{OC}) in photovoltaic devices.

BHJ photovoltaic were fabricated from the terpolymers [ITO/MoOx (10 nm)/polymer: PC₇₁BM (1:2 wt%)/Al (100 nm)], where the donor-acceptor blends were processed from a chloroform: ODCB solvent mixture. The fluorene bridged polymer (**P5**) based device gave the highest PCE 4.9% with corresponding V_{OC} = 0.88 V, J_{SC} = 9.4 mA/cm² and FF = 59% while **P8** based devices were reported to have given the lowest PCE of 2.9% with corresponding V_{OC} = 0.69 V, J_{SC} = 9.43 mA/cm² and FF = 44%. While the J_{SC} generated from the devices prepared from the two polymers were comparable, the V_{OC} of **P5** based devices was found to be significantly higher than that of the devices prepared from **P8**. The higher V_{OC} of **P5** based devices is in accordance with the deeper HOMO energy level (CV measurement). A high V_{OC} is a typical characteristics of photovoltaic devices based on fluorene based polymers (Yohannes et al., 2004; Zhang et al., 2006;

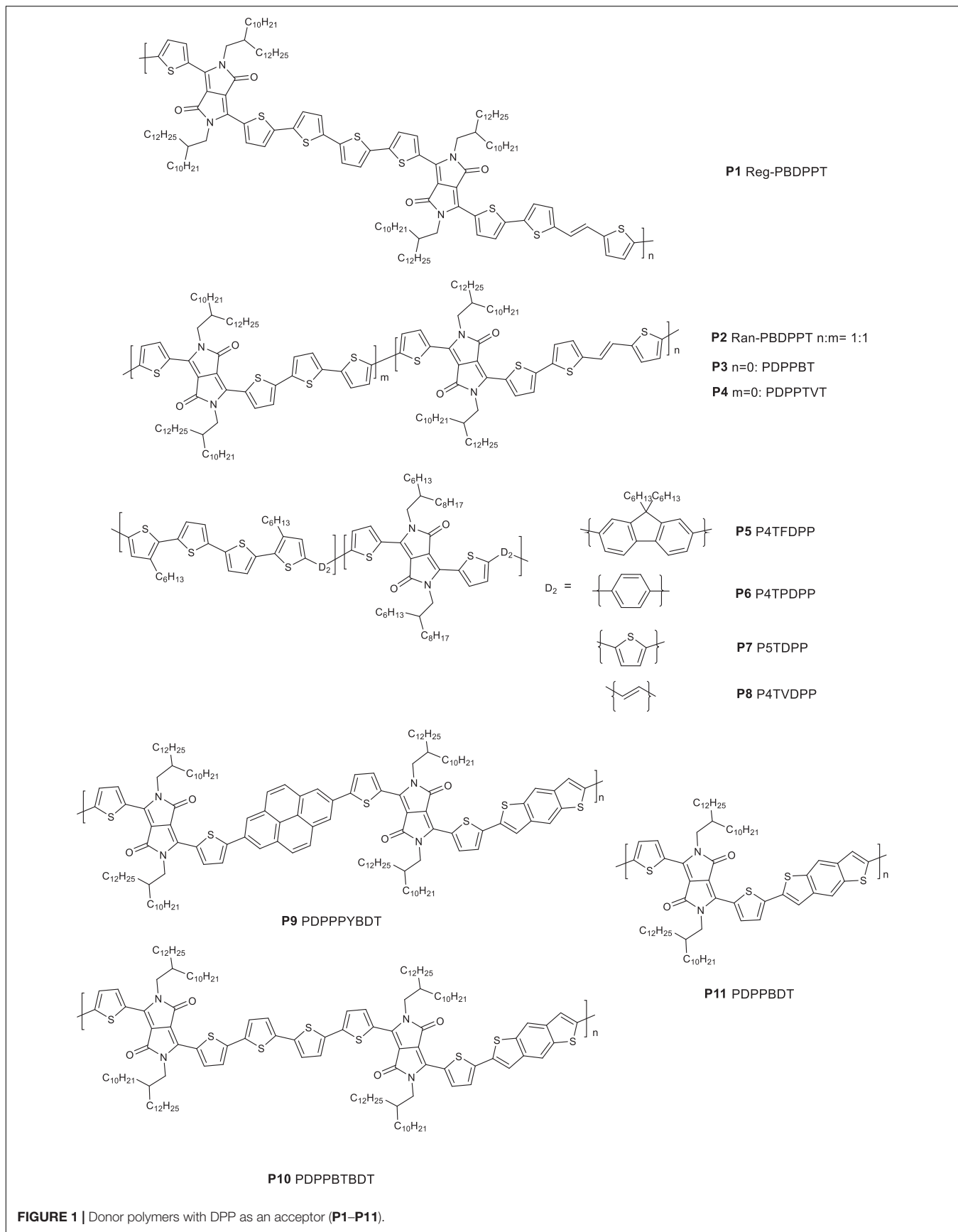


TABLE 1 | Summary of optical, electrochemical, and photovoltaic properties of polymers (**P1–P17**).

Polymer	λ_{onset} (nm)	HOMO (eV)	LUMO (eV)	J_{SC} (mA/cm ²)	V_{OC} (V)	FF (%)	PCE (%)	Acceptor	References
P1	871	−5.25	−3.83	12.29	0.62	71	5.45	PC ₇₁ BM	Ko et al., 2015
P2	878	−5.29	−3.88	13.18	0.61	65	5.24	PC ₇₁ BM	Ko et al., 2015
P3	–	–	–	11.60	0.58	69	4.66	PC ₇₁ BM	Ko et al., 2015
P4	–	–	–	9.40	0.59	69	3.84	PC ₇₁ BM	Ko et al., 2015
P5	–	−5.46	−3.75	9.4	0.88	59	4.9	PC ₇₁ BM	SambathKumar et al., 2016
P6	–	−5.25	−3.79	10.05	0.72	50	3.8	PC ₇₁ BM	SambathKumar et al., 2016
P7	–	−5.11	−3.85	8.57	0.77	61	4.1	PC ₇₁ BM	SambathKumar et al., 2016
P8	–	−5.04	−3.82	9.43	0.69	44	2.9	PC ₇₁ BM	SambathKumar et al., 2016
P9	783	−5.40	−3.82	12.01	0.72	52	4.46	PC ₇₁ BM	Kim et al., 2018
P10	845	−5.33	−3.86	9.31	0.60	54	3.02	PC ₇₁ BM	Kim et al., 2018
P11	830	−5.35	−3.86	7.25	0.66	49	2.36	PC ₇₁ BM	Kim et al., 2018
P12	800	−5.43	−3.58	13.9	0.96	68.34	9.10	<i>m</i> -ITIC	Chen et al., 2017
P13	800	−5.42	−3.57	17.12	0.93	69.26	11.02	<i>m</i> -ITIC	Chen et al., 2017
P14	800	−5.36	−3.52	14.97	0.91	65.66	8.95	<i>m</i> -ITIC	Chen et al., 2017
P15	800	−5.22	−3.38	14.40	0.91	62.14	8.13	<i>m</i> -ITIC	Chen et al., 2017
P16	593	−5.76	−3.73	2.7	0.89	56	1.4	PC ₇₁ BM	Gedefaw et al., 2017b
P17	580	−5.85	−3.73	6.9	0.91	63	3.9	PC ₇₁ BM	Gedefaw et al., 2017b

Gedefaw et al., 2009). Optimized devices fabricated based on **P6** and **P7** gave a PCE of 3.8 and 4.1%, respectively.

The terpolymers were generally found to be less ordered (X-Ray diffraction (XRD) measurement) with a weak diffraction peak and a wider *d*-spacing. However, the vinyl bridged terpolymer (**P8**) showed a stronger diffraction pattern, a higher aggregation tendency and excessive phase separation in the blend films with PC₇₁BM. However, the hole mobility was found to decrease in the order of **P5** > **P7** > **P6** > **P8**. **P5** showed better miscibility with fullerene (AFM image) which supports the reason why the device showed higher PCE in photovoltaics, in contrary to **P8** based devices (rough surface morphology) and lower photovoltaic performances.

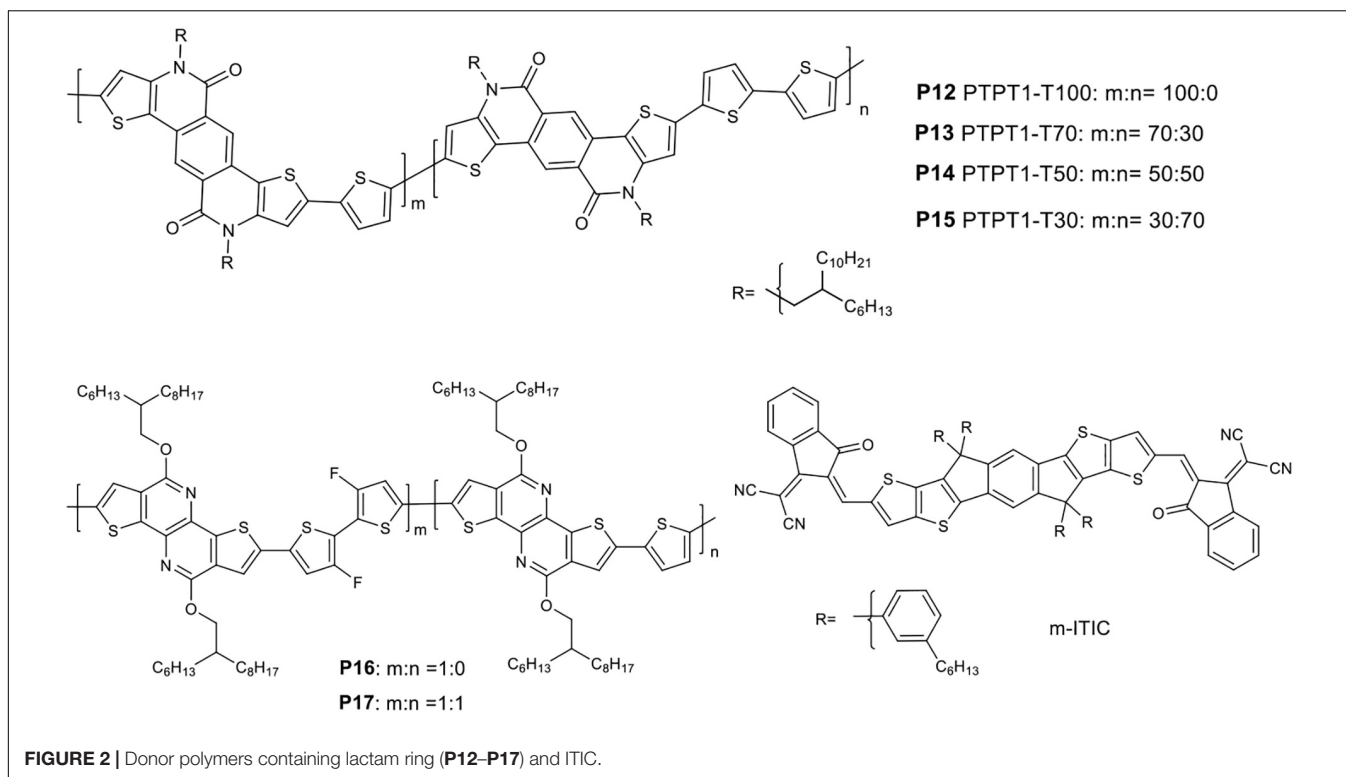
Pyrene and benzodithiophene (BDT) have been extensively studied as electron rich core units in alternating polymers (Beimling and Koßmehl, 1986; Hou et al., 2008; Bolognesi et al., 2013; Gedefaw et al., 2017a; Alkan et al., 2020). Pyrene and bithiophene based monomers were used as a third component together with BDT and DPP based monomers to form two regular terpolymers, denoted as **P9** PDPPPYBDT and **P10** PDPPBTD. Alternating polymers based on DPP and BDT (**P11** PDPPBDT) was also reported (Kim et al., 2018; **Figure 1**). Regular terpolymers have an advantage of having defined chemical compositions compared to random terpolymers (Hendriks et al., 2013). The onset and the peak optical absorption wavelengths of **P11** fell between those of pyrene (**P9**) and bithiophene (**P10**) based terpolymers. In both liquid and solid state, the absorption peak of the pyrene (**P9**) containing terpolymer displayed a blue shift compared to the bithiophene (**P10**) terpolymer. This is expected as the bithiophene molecular unit has a strong electron donating characteristic that shifts absorption to a longer wavelength. The HOMO and LUMO energy levels of **P11** was slightly up shifted (−5.35/−3.86) compared to the values of **P9** (−5.40/−3.82) and **P10** (−5.33/−3.86). The HOMO of **P10** is slightly raised

due to the stronger electron donating effect of bithiophene compared to **P9**. A conventional BHJ solar cells were fabricated (ITO/PEDOT:PSS/polymer: PC₇₁BM/LiF/Al). Hence, a PCE of 4.46, 3.02, and 2.36% were reported from **P9**, **P10**, and **P11**-based devices, respectively, using a mixture of chloroform and ODCB (2:1 v/v) with the addition of 3% DIO solvent and further annealing at 180°C. **P9** based devices gave improved J_{SC} (12.1 mA/cm²) due to the uniform morphology and well-defined nanophase segregation and higher PCE. Moreover, **P9**-based device gave relatively higher V_{OC} .

D-A polymers with multicyclic lactam aromatic systems show extended conjugation length, reduced band gap, enhanced π -electron delocalization, strong π - π stacking, and high hole mobility (Cao et al., 2013, 2015; Kroon et al., 2015). Random terpolymers containing a fused penta cyclic lactam ring, thiophene and bithiophene were reported to modulate molecular packing and nanophase blending in devices (Chen et al., 2017). The terpolymers prepared are denoted as **P12** PTPTI-T100, **P13** PTPTI-T70, **P14** PTPTI-T50, and **P15** PTPTI-T30 consisting of 100, 70, 50, and 30% of the thiophene-lactam block, respectively (**Figure 2**).

m-ITIC (Yang et al., 2016; **Figure 2**) was blended with the donor polymers for fabricating solar cells. The UV-visible absorption spectrum of the polymers blended with ITIC were found to be comparable except for the stronger absorption bands observed for the **P13**:*m*-ITIC blend, which could contribute toward a higher J_{SC} of the devices. The HOMO energy levels of the polymers were determined using ultraviolet photoelectron spectroscopy (UPS). The HOMO of the polymers shifts upward as the amount of thiophene is decreasing. Hence, the deepest HOMO was observed for **P12** (−5.43 eV) while **P15** (−5.22 eV) showed a raised HOMO energy level. The HOMO and LUMO values of *m*-ITIC are −5.50 and −3.92 eV, respectively.

To evaluate the photovoltaic properties, a device structure of ITO/ PEDOT:PSS/active layer/PDINO (Zhang et al., 2014)/Al



was used and film was processed from chlorobenzene: chloroform: DIO (1:2:0.5 vol%). **P12**:*m*-ITIC based device showed a PCE of 9.10% with corresponding $J_{SC} = 13.9 \text{ mA/cm}^2$, $V_{OC} = 0.96 \text{ V}$, and $FF = 68.34\%$. **P13**:*m*-ITIC-based device on the other hand exhibited an impressive PCE of 11.02%, $J_{SC} = 17.12 \text{ mA/cm}^2$, $FF = 69.26\%$, and a $V_{OC} = 0.93 \text{ V}$. The higher J_{SC} achieved from the **P13**:*m*-ITIC-based device could be attributed to: (i) the stronger absorption bands of the blend, (ii) finely distributed microstructure with a small domain size and an increased fraction of face-on oriented crystallites, (iii) a relatively balanced hole and electron mobility. Further increase in the content of the bithiophene monomer (**P14** and **P15**) resulted in a decrease in the PCE (8.95% for **P14** and 8.13% for **P15**).

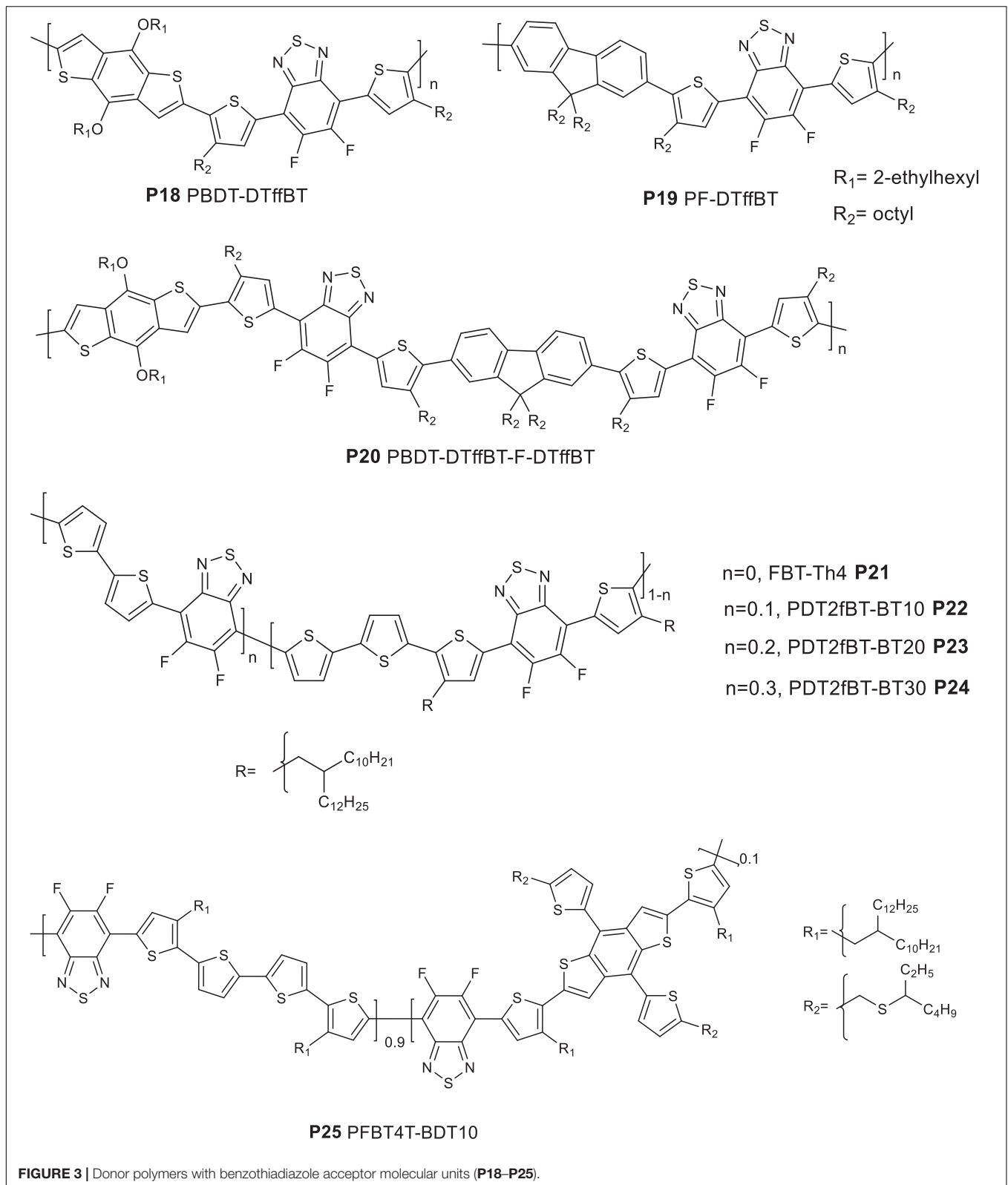
Pyridopyridinedithiophene is another penta cyclic lactam ring derivative copolymerized with thiophene monomer to yield a medium band gap polymer (PTNT) (Kroon et al., 2014). A blend of PTNT:fullerene based solar cell gave a V_{OC} of 0.9 V, a FF of 60% and a PCE of 5% for >200 nm thick active layer. The introduction of fluorine atom in the backbone of a polymer increases planarity and improves hole mobility (Li et al., 2011; Bronstein et al., 2013). Hence, a fluorine atom modified 2,2-bithiophene based monomer was copolymerized with pyridopyridinedithiophene based unit to yield an alternating polymer (**P16**) (Figure 2). However, **P16** had poor solubility in solvents, resulting in a premature precipitation during the polymerization. The devices prepared from a blend of **P16** and PC₇₁BM gave only 1.4% PCE with low J_{SC} and FF though the V_{OC} was respectable (~0.9 V). The film was rough (AFM investigation) due to the severe phase segregation of

the polymer chains and PC₇₁BM. A random terpolymer (**P17**) consisting difluoro-2,2'-(bithiophene) (25%), thiophene (25%) and pyridopyridinedithiophene (50%) molar amounts in the feed of the polymerization was synthesized to improve processability, miscibility, optical and electrochemical properties (Gedefaw et al., 2017b). As presumed, **P17** showed an excellent solubility giving rise to a decent molecular weight (number average 17.2 KDa). The absorption onset of **P16** and **P17** at solid state was found to be 610 and 585 nm, respectively: both are red shifted compared to the reference polymer (PTNT) ($\lambda_{onset} = 560 \text{ nm}$), which could be due to the rigid bithiophene unit. **P17** showed good film making property and hence a smooth surface with smaller root-mean-square roughness (rms) film was obtained when blended with PC₇₁BM (1:2.5 w/w). As the result, **P17**-based photovoltaic devices gave more than 2 times higher PCE than the **P16** based devices (Table 1).

Difluorobenzothiadiazole Ring Based Polymers

In 2011, Li et al. (2011) incorporated difluorobenzothiadiazole as an acceptor together with BDT based donor monomer to make a D-A polymer that gave a 3.4% PCE in photovoltaics. Thereafter, several efficient polymers containing difluorobenzothiadiazole were developed and characterized (Stuart et al., 2013; Wang et al., 2013; Duan et al., 2015).

Deng et al. (2015) reported a regular terpolymer (**P20**) PBDDT-DTffBT-F-DTffBT based on BDT, fluorene and difluoro benzothiadiazole based monomers. By incorporating a weak electron donating fluorene based monomer as a third component,



the molecular energy level and optical absorption were tuned. Reference polymers (**P18** PBBDT-DTffBT and **P19** PF-DTffBT) (Deng et al., 2015; **Figure 3**) were also reported.

The solid state onset of absorption was estimated to be 725, 602, and 696 nm for **P18**, **P19**, and **P20**, respectively. The HOMO and LUMO energy levels were calculated to be $-5.46/-3.75$,

−5.53/−3.47, and −5.47/−3.69 eV for **P18**, **P19**, and **P20**, respectively (CV measurement). Clearly, the optical behavior and molecular energy levels of the terpolymer are intermediate between the properties displayed with **P18** and **P19**. For instance, the HOMO of **P20** was deeper, which is beneficial for achieving higher V_{OC} in solar cell devices than **P19**. The LUMO of the terpolymer is slightly raised than **P18**. A moderate 2.6% PCE was generated [glass/ITO/PEDOT:PSS/polymer:PC₇₁BM (1:1.5 wt/wt)/LiF/Al] from a blend of **P20** and PC₇₁BM, processed using chlorobenzene and 3% DIO. **P18** and **P19** based solar cells gave a PCE of 3.0 and 0.5%. Though the V_{OC} and J_{SC} of **P20** based solar cells was improved, the FF (39.8%) were lower compared to the **P18** based devices (FF = 55.8%). The lower FF of **P20** based devices could have arisen from a poor film morphology and lower hole mobility compared to the films prepared **P18**.

In another work, terpolymers based on difluorobenzothiadiazole, bithiophene and 5,6-difluoro-2,1,3-benzothiadiazole (FBT) (**P21** FBT-Th4, **P22** PDT2fBT-BT10, **P23** PDT2fBT-BT20, and **P24** PDT2fBT-BT30) with 0, 10, 20, and 30%, respectively of bithiophene-FBT segment have been reported (Figure 3; Shin et al., 2018). The FBT unit was used as a third component to reduce the aggregation tendency of the highly crystalline reference polymer (**P21**). The polymers have comparable peak absorption and onset of absorption wavelengths. However, **P22** showed a stronger absorption intensity at longer wavelength, which could be due to the better solubility in chlorobenzene and acetonitrile (AcCN) co-solvents. A downward shift in the HOMO energy level (CV) was observed with the increase in FBT content: **P21** (−5.35 eV) > **P22** (−5.42 eV) > **P23** (−5.43 eV) > **P24** (−5.44 eV). Consequently, a 0.2 cm² solar cell device fabricated based **P22** gave a PCE of 10.31%, J_{SC} of 18.92 mA/cm², FF of 73.45%, and V_{OC} of 0.742 V (ITO/PEI ethoxylated/polymer:PC₇₁BM/MoO₃/Ag). Further increase of the device area to 1.0 cm² resulted a PCE of 9.03%. The high PCE of **P22** based devices is due to the improved processability, crystallinity and morphology. Conversely, optimized solar cell devices fabricated based on **P21**, **P23**, and **P24** yielded a PCE of 8.62, 9.28, and 8.02%, respectively.

A random terpolymer (**P25** PFBT4F-BDT10) (Figure 3; Qing et al., 2020) using 2D-BDT, bithiophene and 5,6-difluorobenzothiadiazole (FBT) based monomers was reported. The bithiophene and BDT monomers were mixed in 0.9–0.1 molar ratio, respectively, in the feed of the polymerization reaction. **P25** showed an absorption peak at 633 nm and a

moderate shoulder at 687 nm. The HOMO energy level was found to be −5.47 eV (CV) while the LUMO (−3.83 eV) was estimated from the optical band gap and the HOMO. A blend of **P25**:PC₇₁BM delivered a PCE of 2.40%, with a V_{OC} of 0.76 V, a J_{SC} of 5.87 mA/cm², and a FF of 53.8% (ITO/ZnO/polymer interlayer/active layer/MoO₃/Al). The lower performance was probably because of the poor BHJ morphology and the poor compatibility of **P25** and PC₇₁BM. In order to modulate the morphology, a ternary blend of **P25**, IDIC and PC₇₁BM was used. A 0.6:1 (wt/wt) of IDIC and PC₇₁BM blend together with **P25** gave over 10% PCE with a V_{OC} = 0.75 V, J_{SC} = 21.12 mA/cm² and FF = 63.9%. The ternary blend gave broader absorption, favorable phase separation, and stronger crystallinity induced by the synergistic effect of the acceptors. Further increase in the content of IDIC, the FF of the devices showed improvement. For instance, a 1:0.6 mixture of IDIC: PC₇₁BM based device showed a FF = 68.2%. However, the J_{SC} dropped to 17.80 mA/cm² and hence the PCE decreased to 9.27%. Table 2 summarizes the properties of **P18**–**P25**.

Benzodithiophenedione (BDD) and Thienopyrroledione (TPD) Rings Based Polymers

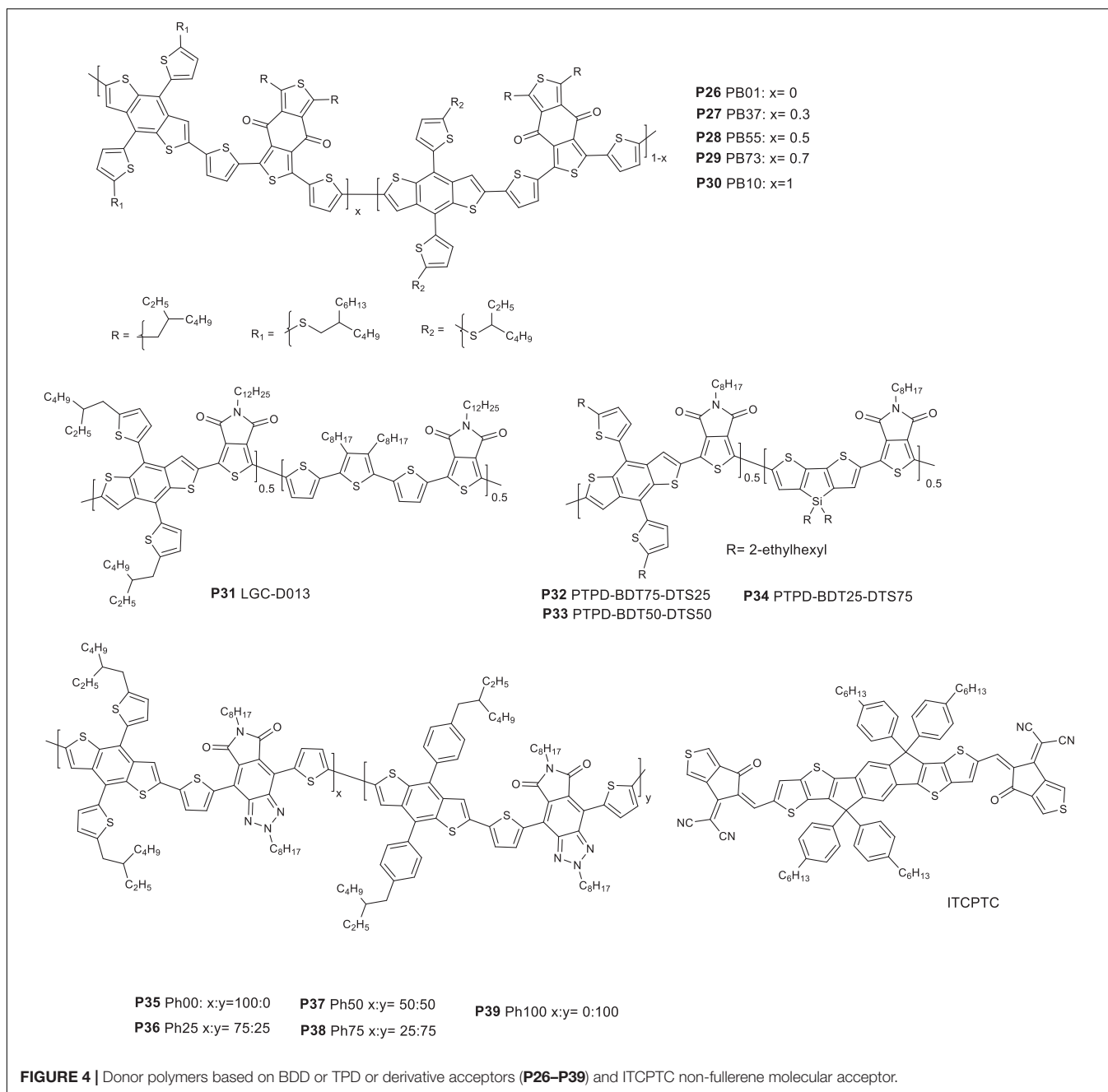
The BDD molecular acceptor have a large planar structure, strong electron-withdrawing ability and high aggregation tendency and polymers based on BDD show high PCE in solar cells (Qian et al., 2012; Huo et al., 2015; Zhang et al., 2017). Aromatic π -bridges such as thiophene can be attached to the BDD unit easily to extend conjugation and control the backbone twisting (Ie et al., 2012; Qian et al., 2012). Here, the most recent BDD based terpolymers developed are summarized.

A series of polymers with two electron rich 2D-BDT and BDD based monomers are reported. The BDT based monomers have a thiol alkyl chains differing in the length of the alkyl groups (butyl octyl versus ethyl hexyl). The polymers are represented as **P26** PB01, **P27** PB37, **P28** PB55, **P29** PB73, and **P30** PB10 with 0, 30, 50, 70, and 100% of the BDTBO-BDD (BDTBO: butyl octyl side chain on the BDT) segment, respectively (Figure 4; Huo et al., 2018).

Bands at 300–400 and 500–700 nm corresponding to a π - π^* transition and intramolecular charge transfer (ICT), respectively, are displayed in the UV-visible spectrum. The polymers showed similar optical band gaps (in the range of 1.83 and 1.85 eV)

TABLE 2 | Summary of optical, electrochemical, and photovoltaic properties of polymers (**P18**–**P25**).

Polymer	λ onset (nm)	HOMO (eV)	LUMO (eV)	J_{SC} (mA/cm ²)	V_{OC} (V)	FF (%)	PCE (%)	Acceptor	References
P18	725	−5.46	−3.75	7.33	0.733	55.8	3.0	PC ₇₁ BM	Deng et al., 2015
P19	602	−5.53	−3.47	2.21	0.649	31.9	0.5	PC ₇₁ BM	Deng et al., 2015
P20	696	−5.47	−3.69	7.48	0.865	39.8	2.6	PC ₇₁ BM	Deng et al., 2015
P21	765	−5.35	−3.73	16.48	0.753	69.52	8.62	PC ₇₁ BM	Shin et al., 2018
P22	767	−5.42	−3.80	18.92	0.742	73.45	10.31	PC ₇₁ BM	Shin et al., 2018
P23	756	−5.43	−3.79	18.46	0.719	69.73	9.28	PC ₇₁ BM	Shin et al., 2018
P24	757	−5.44	−3.80	16.00	0.724	69.21	8.02	PC ₇₁ BM	Shin et al., 2018
P25	775	−5.47	−3.83	21.12	0.75	63.9	10.17	IDIC: PC ₇₁ BM	Qing et al., 2020



in solid state, apart from slight variations in the absorption intensity caused by the difference in their aggregation tendency. The HOMO/LUMO energy levels (CV) of **P26**, **P27**, **P28**, **P29**, and **P30** were calculated to be $-5.40/-3.54$, $-5.42/-3.56$, $-5.44/-3.57$, $-5.44/-3.59$, and $-5.46/-3.60$ eV, respectively. A downward shift in the energy levels was observed as the content of the BDT monomer with the BO alkyl group increases which could be due to the improved solubility, reduced chain aggregation and hence minimizing the aggregation initiated upward shift of the molecular energy levels (Heuvel et al., 2018). Finally, solar cell devices were prepared (ITO/PEDOT:PSS/active layer/ZrAcac/Al) by blending the polymers with either PC₇₁BM

or ITCPTC. A blend of **P28** and ITCPTC acceptor (**Figure 4**) gave an impressive PCE of 12.1% with a corresponding $J_{SC} = 17.0$ mA/cm², $V_{OC} = 0.93$ V, and FF = 74.8%. The devices prepared based on **P26**, **P27**, **P29**, and **P30** yielded a PCE of 10.3, 11.0, 11.0, and 10.1%, respectively, when blended with ITCPTC. The use of PC₇₁BM yielded a slightly lower PCE as indicated in **Table 3**. In both acceptor types, **P28** outperformed due to its enhanced optical absorption and fine-tuned electrochemical and morphological properties.

Another versatile aromatic structure molecular with two imide functional groups, easy synthesis and provides structural flexibility is TPD (Zou et al., 2010; Bang et al., 2017;

TABLE 3 | Summary of optical, electrochemical, and photovoltaic properties of polymers (**P26–P39**).

Polymer	λ onset (nm)	HOMO (eV)	LUMO (eV)	J_{SC} (mA/cm ²)	V_{OC} (V)	FF (%)	PCE (%)	Acceptor	References
P26	–	–5.40	–3.54	12.6	0.92	76.0	8.8	PC ₇₁ BM	Huo et al., 2018
P27	–	–5.42	–3.56	13.5	0.91	73.1	8.9	PC ₇₁ BM	Huo et al., 2018
P28	–	–5.44	–3.57	13.7	0.94	76.5	9.9	PC ₇₁ BM	Huo et al., 2018
P29	–	–5.44	–3.59	13.2	0.92	72.0	8.7	PC ₇₁ BM	Huo et al., 2018
P30	–	–5.46	–3.60	13.3	0.92	68.6	8.4	PC ₇₁ BM	Huo et al., 2018
P26	–	–	–	15.3	0.91	72.3	10.1	ITCPT	Huo et al., 2018
P27	–	–	–	15.9	0.91	72.6	10.5	ITCPT	Huo et al., 2018
P28	–	–	–	17.0	0.93	74.8	11.8	ITCPT	Huo et al., 2018
P29	–	–	–	16.5	0.91	71.6	10.8	ITCPT	Huo et al., 2018
P30	–	–	–	15.6	0.91	68.9	9.8	ITCPT	Huo et al., 2018
P31	673.8	–5.56	–	11.29	0.87	73.13	7.22	PC ₇₁ BM	Bang et al., 2017
P32	689	–5.58	–3.79	10.83	0.94	56.52	5.78	PC ₇₁ BM	Heo et al., 2018
P33	701	–5.50	–3.74	8.17	0.92	46.90	3.52	PC ₇₁ BM	Heo et al., 2018
P34	720	–5.42	–3.70	9.65	0.89	55.01	4.74	PC ₇₁ BM	Heo et al., 2018
P35	673.8	–5.26	–3.11	15.92	0.85	54.82	7.42	ITIC	Li K. et al., 2018
P36	663	–5.29	–3.11	16.11	0.86	59.44	8.23	ITIC	Li K. et al., 2018
P37	656	–5.30	–3.12	15.87	0.87	61.97	8.55	ITIC	Li K. et al., 2018
P38	652.6	–5.32	–3.13	15.45	0.89	56.08	7.71	ITIC	Li K. et al., 2018
P39	652.6	–5.33	–3.15	15.23	0.90	55.58	7.62	ITIC	Li K. et al., 2018

Heo et al., 2018). Terpolymers based on TPD molecular unit have been reported.

Bang et al. (2017) reported a terpolymer based on TPD, BDT and terthiophene molecular structures in a 50, 25, and 25% mixing molar ratio of the monomers, respectively (**P31**) (Figure 4). It showed broad optical absorption (300–700 nm) and a band gap of 1.84 eV. The HOMO energy level of the polymer was estimated to be –5.56 eV (CV). **P31** was tested in photovoltaics (ITO/PEDOT:PSS/**P31** LGCD013:PC₇₁BM/Ca/Al), where **P31** and PC₇₁BM (1:2 wt/wt) is processed with ODCB. As prepared device gave a 6.09% PCE, $V_{OC} = 0.88$ V, $J_{SC} = 9.48$ mA/cm² and FF = 72.55%. The PCE was improved to 7.22% with the addition of 3% DIO as an additive.

Thienyl-substituted BDT, dithieno[3,2-*b*:2',3'-*d*]silole (DTS) and TPD based monomers were used to prepare random terpolymers (**P32** PTPD-BDT75-DTS25, **P33** PTPD-BDT50-DTS50, and **P34** PTPD-BDT25-DTS75) with 25, 50, and 75% of the TPD-DTS segment (Figure 4; Heo et al., 2018). Note that the DTS based monomers are widely known for its relatively simple and symmetrical structure and strong electron-donating ability. D-A polymers based on DTS and TPD were reported in the past and used in solar cell devices (Chu et al., 2011). The polymers showed a red shift in the onset of the optical absorption with the increase of the DTS content. Hence, the onset of absorption **P34** is 720 nm while **P32** and **P33** shown 689 and 701 nm, respectively. The absorption intensity of **P32** (25% of TPD-DTS) was stronger at longer wavelength which indicates its better light harvesting capability while **P34** showed a relatively broader absorption attributed to an enriched – TPD-DTS-TPD-DTS- segment. The HOMO and LUMO energy levels shifted upwards with the increase in DTS content. Therefore, the HOMO energy levels of **P32**, **P33**, and

P34 were estimated to be –5.58, –5.50, –5.42 eV, respectively. Similarly, the LUMO energy levels shifted up wards with the increase in DTS content. Finally, solar cells were fabricated in an inverted configuration (ITO/ZnO/polymer:PC₇₁BM/MoO₃/Ag). The highest PCE achieved were 5.78, 3.52, and 4.74% from **P32**, **P33**, and **P34**, respectively, based devices. The higher PCE **P32** based device was due to the better J_{SC} , V_{OC} , and FF compared to **P33** and **P34** based devices. The higher V_{OC} of **P32** based device is expected as it has a deeper HOMO. Despite the narrower absorption, **P32** based devices gave a better J_{SC} probably due to: (i) the higher hole and electron mobility, (ii) stronger absorption coefficient, and (iii) bicontinuous, uniform and smooth morphology (Kawashima et al., 2015).

4,8-di(thien-2-yl)-6-octyl-2-octyl-5H-pyrrolo[3,4-*f*]benzotriazole-5,7(6H)-dione (TzBI) monomer possesses a TPD-triazole functional group and have a moderate electron-withdrawing ability (Fan et al., 2017). The TZBI acceptor was also combined with variable amount of two BDT based donor monomers (an alkyl thiophene (Th) and an alkyl phenyl (Ph) side groups). The polymers prepared are represented as **P35** Ph00, **P36** Ph25, **P37** Ph50, **P38** Ph75, and **P39** Ph100, where **P35** and **P39** are reference polymer prepared from the BDT-Th and the BDT-Ph based monomers, respectively. In the contrary, **P36**, **P37**, and **P38** have 25, 50, 75% the BDT-Ph-TZBI backbone (Figure 4; Li K. et al., 2018). The peak and onset of absorption blue shifts with the increase in BDT-Ph based monomer content. Hence, the optical band gaps are 1.84, 1.87, 1.89, 1.90, and 1.90 eV for **P35**, **P36**, **P37**, **P38**, and **P39**, respectively. The HOMO energy levels are between –5.26 and –5.33 eV with the deepest given by **P39** while the LUMO are in the range of –3.11 to –3.15 eV. ITIC (Figure 2) was used as an acceptor for the solar cells (ITO/PEDOT:PSS /active layer/(PFN-Br)/Ag). The photoactive layers were spin cast from chlorobenzene with

0.5 vol% dibenzyl ether (DBE) solvent additive and subsequently thermally annealed (120 °C for 10 min). The best PCE recorded were 7.42, 8.23, 8.55, 7.71, and 7.62% for **P35**, **P36**, **P37**, **P38**, and **P39** based devices, respectively. Clearly, the performance showed improvement with the introduction of some amount of phenyl substituted BDT monomer: the highest performance being achieved from **P37** based devices: $V_{OC} = 0.87$ V and FF = 61.97% and $J_{SC} = 15.29$ mA/cm². However, when the content of the BDT-Ph based monomer further increased (**P38** and **P39**), the PCE dropped. It is interesting to note that the terpolymers (**P36**, **P37**, and **P38**) performed better than the binary polymers (**P35** and **P39**) presumably due to the balanced hole and electron mobility and suppressed bimolecular recombination.

Thieno[3,4-b]Thiophene (TT) Ring Based Polymers

The TT molecular unit stabilizes the quinoidal structure and hence its presence in polymer backbones helps to lower band gap. The TT core unit has been widely utilized as an acceptor in D-A polymers (Liang et al., 2009a, BR74). Recently, the TT based acceptor was used for the synthesis of terpolymers and the properties are summarized in **Table 4**. The TT based monomer was copolymerized with DTS and BDT based monomers to give random (**P40** ran-PDTSTTBDT) and regular (**P41** reg-PDTSTTBDT) terpolymers. TT, DTS and BDT based monomeric units were introduced in 50, 25, and 25% molar ratios, respectively, as a feed of the polymerization reaction to form **P40**. **P41** on the other hand was prepared from a copolymerization of BDT-TT-BDT and DTS based monomers (**Figure 5**; Heo et al., 2016). **P40** showed a 24 nm blue shift in the absorption peak compared to that of **P41**. However, **P40** revealed a broader optical absorption covering in the high and low energy regions (Kang et al., 2013; Hendriks et al., 2014). The lower energy broadening is attributed to a TT-DTS-TT-DTS enriched segment while the high energy broadening to TT-BDT-TT-BDT- rich segments in the chain. **P41** exhibited low lying HOMO energy level (−5.19 eV) compared to the **P40** (−5.08 eV) (CV measurement). The higher HOMO of the random copolymer is attributed to the higher content of TT-DTS-TT-DTS rich segments, which would have an impact on the V_{OC} of the solar cell device. The LUMO energy level of both polymers is −3.62 eV. Inverted BHJ PSCs were fabricated (ITO/ZnO/polymer:PC₇₁BM/MoO₃/Ag) to evaluate

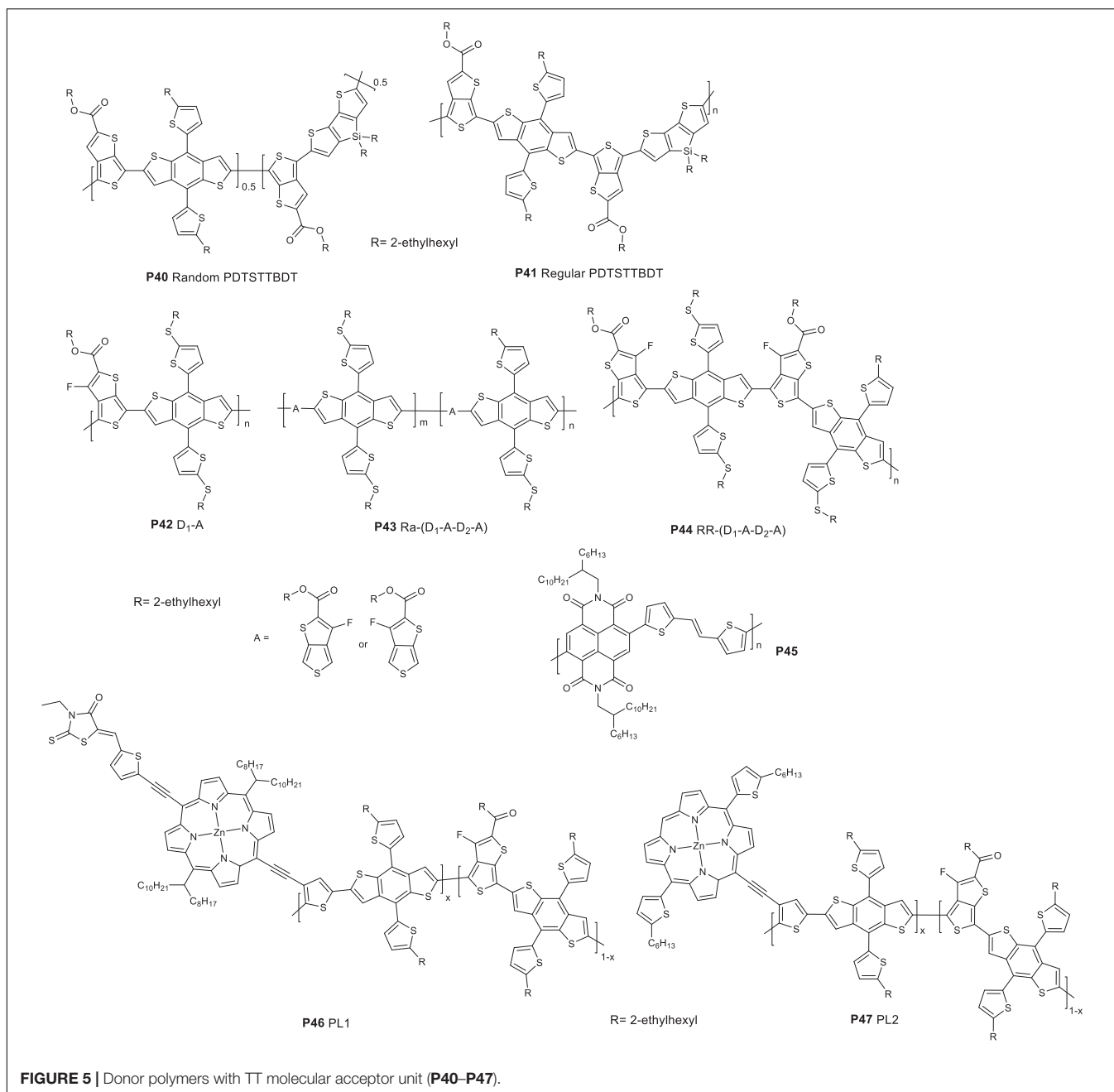
the photovoltaic properties of the polymers. The device based on the **P40** showed a $V_{OC} = 0.50$ V, a $J_{SC} = 5.61$ mA/cm², a FF = 39.19%, and a PCE of 1.11%. However, **P41** based device exhibited remarkably improved PCE with a $V_{OC} = 0.64$ V, a $J_{SC} = 14.35$ mA/cm², a FF = 61.81%, and a PCE of 5.64% with chlorobenzene processing solvent. The PCE of **P41** based devices further increased to 5.75% with the use *o*-xylene and 5% DIO processing solvent. A mixture of 2% p-anisaldehyde (AA) and 3% DIO solvent additive has further increased the PCE to 6.14%. The higher PCE of **P41** based devices is attributed to better crystallinity, higher charge carrier mobility, excellent solubility in solvents, low lying HOMO, bicontinuous interpenetrating network and smoother surface.

Kim et al. (2019) reported terpolymers based on two BDT donor units (thio-2-ethylhexyl substituted BDT and a 2-ethylhexyl-substituted BDT and fluorinated TT denoted as **P43** Ra-(D1-A-D2-A) and **P44** RR-(D1-A-D2-A). A reference polymer (**P42** D1-A) prepared from 2-ethylhexyl-thio-substituted BDT and fluorinated TT based monomers was also reported (**Figure 5**). Regioregular polymer (**P44**) showed a strong absorption coefficient at longer wavelength attributed to the stronger polymer inter-chain interactions, believed to improve light harvesting. On the basis of the electrochemical study, both **P43** and **P44** showed a slight up-shifted HOMO energy levels compared to **P42** which arises from the difference in the composition of the alkyl substituents. An all-PSC was fabricated by blending each of the polymers with **P45** P(NDI2HD-DTAN) (ITO/ZnO/active layer/MoO₃/Ag). A device fabricated from a blend of **P44** and **P45** gave a maximum PCE of 6.13%, $V_{OC} = 0.73$ V, $J_{SC} = 13.59$ mA/cm² and FF = 60%. Devices fabricated based on **P42** or **P43** yielded a PCE of 4.81 and 4.93%, respectively. The high PCE of the device based on **P44** is attributed to the improved charge transport and enhanced light absorption coefficient. **P45** was chosen as an acceptor due to its miscibility with BDT based monomers (Cho et al., 2018).

Random terpolymers (**P46** PL1 and **P47** PL2) possessing fluorinated TT, BDT and thiophene-substituted with porphyrin center were reported (**Figure 5**) Liu Z. et al., 2020). The feed of the porphyrin, BDT and TT containing monomers were in 0.01:1:0.99 molar ratio in the polymer synthesis. The absorption edges of **P46** and **P47** are 816 and 761 nm, respectively. The HOMO of **P46** and **P47** was estimated to be −5.38 and −5.44 eV, respectively. Solar cells were fabricated (ITO/PEDOT:PSS/donor:PC₇₁BM/PFN/Al) that gave 5.73 and

TABLE 4 | Summary of optical, electrochemical, and photovoltaic properties of polymers (**P40–P47**).

Polymer	λ_{onset} (nm)	HOMO (eV)	LUMO (eV)	J_{SC} (mA/cm ²)	V_{OC} (V)	FF (%)	PCE (%)	Acceptor	References
P40	855.1	−5.19	−3.62	5.61	0.50	39.19	1.11	PC ₇₁ BM	Heo et al., 2016
P41	968.6	−5.08	−3.62	14.35	0.64	61.81	5.64	PC ₇₁ BM	Heo et al., 2016
P42	789.7	−5.43	−3.68	12.22	0.74	51	4.81	P45	Kim et al., 2019
P43	789.7	−5.38	−3.63	11.53	0.71	58	4.93	P45	Kim et al., 2019
P44	784.7	−5.38	−3.65	13.59	0.73	60	6.13	P45	Kim et al., 2019
P45	756.0	−5.59	−3.95	–	–	–	–	–	Kim et al., 2019
P46	816	−5.38	−3.60	12.3	0.86	54.4	5.73	PC ₇₁ BM	Liu Z. et al., 2020
P47	761	−5.44	−3.47	15.2	0.84	55.9	7.14	PC ₇₁ BM	Liu Z. et al., 2020



7.14% PCE for the devices based on **P46** and **P47**, respectively, after processing the film with chlorobenzene and 1.5% DIO (v/v).

TERPOLYMERS CONSISTING TWO ACCEPTORS AND ONE DONOR UNITS

Random and regular terpolymers built from two electron-accepting and one electron-rich monomers have been investigated with the objective of optimizing absorption spectra and molecular energy levels. Herein, materials developed recently are discussed.

Quinoxaline Ring Based Polymers

Andersson's research group developed the synthesis of quinoxaline based molecular structures and subsequently incorporated in a wide assortment of D-A polymers for polymer solar cells (Gedefaw et al., 2009; Lindgren et al., 2009; Zhou et al., 2010; Gedefaw et al., 2017a). The quinoxaline molecular system is among the structures used to develop terpolymers and some of the efforts are summarized in this section and the properties are shown in **Table 5**. Suzuki coupling reaction of benzothiadiazole (25%), quinoxaline (25%), and fluorene (50%) based monomers yielded a random terpolymer (**P49**) (**Figure 6**). A reference polymer based

TABLE 5 | Summary of optical, electrochemical, and photovoltaic properties of polymers (P48–P55).

Polymer	λ onset (nm)	HOMO (eV)	LUMO (eV)	J_{SC} (mA/cm ²)	V_{OC} (V)	FF (%)	PCE (%)	Acceptor	References
P48	630	−5.7	−3.3	7.78	0.82	50	3.18	PC ₇₁ BM	Gedefaw et al., 2016a
P49	630	−5.7	−3.3	5.97	0.84	42	2.14	PC ₇₁ BM	Gedefaw et al., 2016a
P50	760	−5.87	−3.97	8.9	0.79	64	4.5	PC ₆₁ BM	Seri et al., 2017
P51	925.3	−5.23	−3.60	13.88	0.83	64	7.37	PC ₇₁ BM	Keshtov et al., 2019
P52	953.7	−5.24	−3.63	14.36	0.83	66	7.87	PC ₇₁ BM	Keshtov et al., 2019
P53	1068.8	−5.26	−3.67	15.74	0.86	68	9.20	PC ₇₁ BM	Keshtov et al., 2019
P54	1078	−5.28	−3.70	14.78	0.88	66	8.58	PC ₇₁ BM	Keshtov et al., 2019
P55	1087.6	−5.30	−3.73	14.08	0.90	64	8.11	PC ₇₁ BM	Keshtov et al., 2019

on quinoxaline and fluorene monomers was also reported (P48) (Gedefaw et al., 2016a). P49 has revealed an extended and broad optical absorption spectrum, showing the role of the third component (benzothiadiazole) in fine tuning the optical absorption. The HOMO and LUMO energy levels of both polymers were estimated to be −5.7 and −3.3 eV (CV). The photovoltaic properties of the polymers were studied (glass/ITO/PEDOT:PSS/Polymer:PC₇₁BM (1:4 wt/wt) /LiF/Al). P49 based device gave a PCE of 2.14% while P48 based devices gave a higher PCE (3.18%) when the films are processed with ODCB. The lower performance of P49 based devices is due to the lower J_{SC} and FF, attributed to the higher content of the third component (25%) which results in polymer chain twisting and likely causing excessive miscibility of the polymer with the acceptor.

In another work, a regular terpolymer (P50 PBTDQx-ii) based on fluorinated quinoxaline, isoindigo and BDT monomers was reported (Figure 6; Seri et al., 2017). P50 showed a 760 nm onset of absorption at solid state. A D-A polymer prepared from the quinoxaline and BDT based monomers was reported to have an absorption onset of 714 nm (Tessarolo et al., 2014). The HOMO and LUMO energy levels of P50 was estimated to be −5.87 and −3.97 eV, respectively (CV). The photovoltaic property of the polymer was probed in a glass/ITO/ZnO/active layer/ MoO₃/Ag structure. A 1:2 wt/wt blend of P50 and PC₆₁BM processed with *o*-xylene and 3% DIO with the films prepared by blade coating technique gave a 4.5% PCE, J_{SC} = 8.9 mA/cm², V_{OC} = 0.79 V and FF = 64%. For comparison, a PCE of 4.0% was achieved when the film is processed with ODCB.

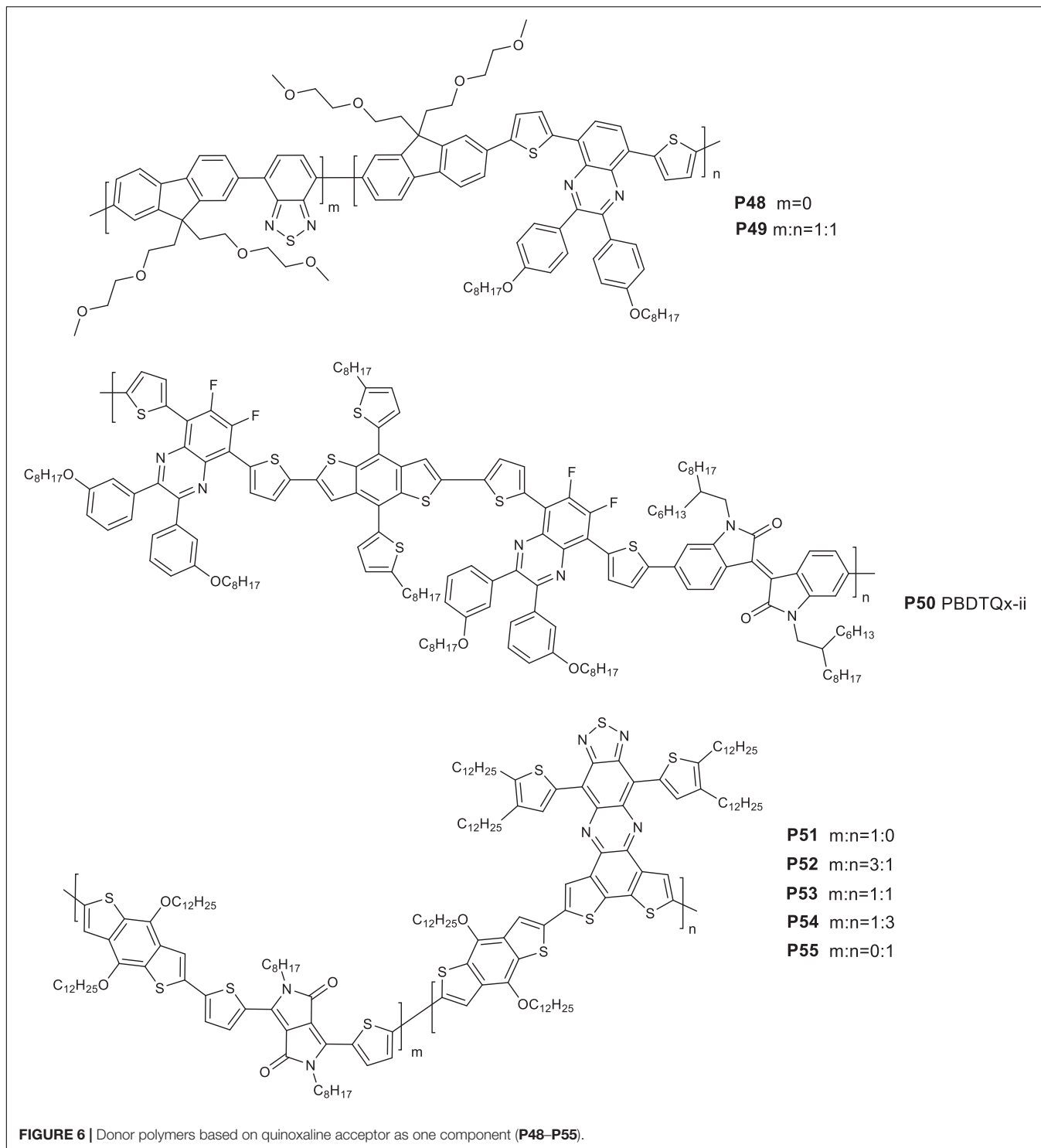
A series of terpolymers (P51–P55) (Figure 6) were synthesized by mixing different feed amounts of monomers based on benzothiadiazolequinoxaline (BTQx), DPP and BDT based molecular units (Keshtov et al., 2019). P51 and P55 are reference polymers with no BTQx and DPP, respectively. P52, P53, and P54 are random terpolymers composed of the BDT-DPP and BDT-BTQx segments in 3:1, 1:1, and 1:3 ratios, respectively. The polymers were blended with PC₇₁BM to fabricate solar cells (ITO/PEDOT:PSS/active layer/PFN/Al). P53 showed excellent light collecting ability, high charge-carrier mobility, and a low-lying HOMO energy level and hence P53 based device exhibited a V_{OC} = 0.86 V, J_{SC} = 15.74 mA/cm², and FF = 68%, leading to a PCE = 9.20%: higher than the PCE achieved from P51 (7.37%) and

P55 (8.11%). P52 and P54 based devices gave a PCE of 7.87 and 8.58%.

Difluorobenzothiadiazole Ring Based Polymers

Table 6 summarizes the properties of terpolymers based on difluorobenzothiadiazole acceptor. Duan et al. (2016) synthesized random terpolymers using 5,6-difluoro-4,7-dithieno[2,1,3]thiadiazole (DTfBT), 5,6-difluorobenzo[2,1,3]thiadiazole (fBT), and thienyl-substituted benzo[1,2-b:4,5-b']dithiophene (BDT): P56 Th00, P57 Th25, P58 Th35, and P59 Th100 (the BDT monomer has a *n*-decyl alkyl side chain in P59). P56 and P59 are reference polymers based on fBT-BDT and DTfBT-BDT segments, respectively. P57 and P58 are random polymers consisting of 25 and 35% of the DTfBT-BDT segment, respectively (Figure 7; Duan et al., 2016). The onset of absorption is the same for all polymers while the absorption maxima of P57 and P58 lie between P56 and P59. Similarly, the polymers showed ideal molecular energy levels and within the same range. Promising PCE of 8.0 and 7.9% were achieved from the P57 and P58 based solar cell devices, respectively, higher than the devices fabricated based on P56 (PCE = 4.9%) and P59 (PCE = 6.9%).

To further understand the effect of electronegative atoms, random terpolymers were reported: P58 P2TBT-BT, P60 P2TBX-BT, P61 P2TBT-BX, and P62 P2TBX-BX (Liu et al., 2019). P58 P2TBT-BT is the same as Th35 reported earlier (Duan et al., 2016). Contrary, P62 is a difluorobenzoxadiazole (BX) analog of P58 (sulfur is replaced with oxygen). P60 and P61 have both BT and BX units in their backbones (Figure 7). The polymers showed an absorption maxima between 658 nm and 662 nm while the absorption onsets are between 730 nm and 734 nm (Wang et al., 2017). However, differences in the molecular energy levels (CV study) have been noticed: the LUMO energy level shifted downward going from P58 to P62 which could be due to the stronger electron negativity of BX compared to BT (oxygen is more electronegative than sulfur). A similar trend was observed with the HOMO energy level, however, the change was small compared to the LUMO. In the photovoltaic properties study (ITO/PEDOT:PSS/polymers:PC₇₁BM/ PFN-Br/Ag), the PCEs generated were 8.8, 7.9, 7.0, and 6.7% from P58, P60, P61, and P62 based devices, respectively. With the introduction of BX, the PCE decreased due to the decrease in J_{SC} even though the



V_{OC} slightly increases. The morphology of the films (GIWAXS and TEM) was similar. PL quenching efficiencies of films are 94, 88, 88, and 82% when **P58**, **P60**, **P61**, and **P62** are blended with PC₇₁BM, respectively, indicating the decrease in the charge transfer efficiencies with the introduction of BX in the polymer backbone, which could be due to the closeness of the LUMO of

the polymers to the LUMO of PC₇₁BM. This explains the decrease in the J_{SC} of the devices with the introduction of BX. On the other hand, **P58** has the most favorable energy level alignment with PC₇₁BM and therefore resulting in a high PCE (8.8%).

4,7-bis(5-bromo-4-(2-octyldodecyl)thiophen-2-yl)-5,6-difluorobenzo[c][1,2,5]thiadiazole, dimethyl-2,2'-(thieno[3,2-b]thioph

TABLE 6 | Summary of optical, electrochemical, and photovoltaic properties of polymers (**P56–P79**).

Polymer	λ onset (nm)	HOMO (eV)	LUMO (eV)	J_{SC} (mA/cm ²)	V_{OC} (V)	FF (%)	PCE (%)	Acceptor	References
P56	729	-5.93	-3.76	8.4	0.91	64	4.9	PC ₇₁ BM	Duan et al., 2016
P57	729	-5.86	-3.72	12.6	0.90	70	8.0	PC ₇₁ BM	Duan et al., 2016
P58	729	-5.85	-3.71	12.3	0.89	72	7.9	PC ₇₁ BM	Duan et al., 2016
P59	721	-5.79	-3.61	12.2	0.84	67	6.9	PC ₇₁ BM	Duan et al., 2016
P58	729.3	-5.45	-3.10	13.8	0.88	73	8.8	PC ₇₁ BM	Liu et al., 2019
P60	729.3	-5.52	-3.40	12.5	0.88	72	7.9	PC ₇₁ BM	Liu et al., 2019
P61	733.6	-5.56	-3.50	12.9	0.91	60	7.0	PC ₇₁ BM	Liu et al., 2019
P62	733.6	-5.58	-3.53	11.7	0.93	61	6.7	PC ₇₁ BM	Liu et al., 2019
P63	751	-5.30	-3.66	19.0	0.744	73.5	10.39	PC ₆₁ BM	Xie et al., 2019
P64	747	-5.39	-3.74	18.6	0.745	75.2	10.42	PC ₆₁ BM	Xie et al., 2019
P65	742	-5.41	-3.74	16.6	0.718	75.0	8.94	PC ₆₁ BM	Xie et al., 2019
P66	756	-5.34	-3.69	18.5	0.79	71	10.3	PC ₇₁ BM	Ma et al., 2015
P67	742	-5.39	-3.67	11.08	0.86	64	6.12	PC ₇₁ BM	Tang et al., 2019
P68	882	-5.37	-3.59	12.52	0.75	68	6.41	PC ₇₁ BM	Tang et al., 2019
P69	912	-5.35	-3.66	9.61	0.73	68	4.82	PC ₇₁ BM	Tang et al., 2019
P70	946	-5.35	-3.68	6.68	0.75	71	3.57	PC ₇₁ BM	Tang et al., 2019
P71	923	-5.34	3.78	7.87	0.73	66	3.80	PC ₇₁ BM	Tang et al., 2019
P72	-	-4.90	-3.33	19.17	0.903	70.9	12.27	ITCPTC _{0.7} :meta-TrBRCN _{0.3}	Xu et al., 2019a
P73	-	-4.88	-3.35	20.16	0.886	76.3	13.63	ITCPTC _{0.7} :meta-TrBRCN _{0.3}	Xu et al., 2019a
P74	-	-4.86	-3.35	19.49	0.877	74.4	12.72	ITCPTC _{0.7} :meta-TrBRCN _{0.3}	Xu et al., 2019a
P75	795	-5.23	-3.67	18.19	0.732	71	9.76	PC ₇₁ BM	Rasool et al., 2019
P76	795	-5.24	-3.68	18.13	0.726	70	9.59	PC ₇₁ BM	Rasool et al., 2019
P77	795	-5.27	-3.71	17.89	0.736	71	9.66	PC ₇₁ BM	Rasool et al., 2019
P78	795	-5.27	-3.71	15.23	0.729	65	7.47	PC ₇₁ BM	Rasool et al., 2019
P79	795	-5.28	-3.72	14.75	0.724	64	7.12)	PC ₇₁ BM	Rasool et al., 2019

ene-2,5-diyl)bis(thiophene-3-carboxylate) (4T2C) and bithiophene were reacted together to yield three random terpolymers: **P63** PffBT4T-4T2C-19/1, **P64** PffBT4T-4T2C-9/1, and **P65** PffBT4T-4T2C-4/1 (Xie et al., 2019). An alternating polymer was prepared by the polymerization of 4,7-bis(5-bromo-4-(2-octyldecyl)thiophen-2-yl)-5,6-difluorobenzo[c][1,2,5]thiadiazole and 5,5'-bis(trimethylstannyl)-2,2'-bithiophene to yield **P66** PffBT4T-2OD (Ma et al., 2015; **Figure 7**). The content of the 4T2C monomer increases going from **P63** to **P64** to **P65**. The optical absorption of the terpolymers were tuned by varying the composition of the monomers introduced in the chain. Hence, a higher content of the 4T2C monomer resulted in the weakening of the absorption peak intensity at ~680 nm indicating the reduction of the intermolecular polymer chain interactions. However, generally a strong polymer aggregation was observed even in solution and at room temperature. The HOMO of the polymers shifts downward with the increase in the 4T2C content (CV). The polymers were used in solar cells (ITO/PEDOT:PSS/ (polymer:PC₆₁BM)/bis-C60/Ag or an inverted structure of ITO/ZnO/polymer:PC₆₁BM:MoO₃/Ag. **P63** based devices gave a PCE of 9.29%, $J_{SC} = 16$ mA/cm², $V_{OC} = 0.772$ V and FF = 75.2% in a conventional device processed without DIO. With the increase in the 4T2C unit (**P64**), the PCE increased to 9.61%, $J_{SC} = 15.5$ mA/cm², $V_{OC} = 0.784$ V and FF = 79.1%. Further increase in the 4T2C unit, the PCE lowered to 7.47%. With the addition of 3% DIO and the use inverted structure, a PCE of 10.39, 10.42, and

8.94% for **P63**, **P64**, and **P65**, based devices, respectively, were achieved. The highest PCE of the devices based on **P64** was due to the relatively high and balanced hole- electron mobility (hole mobility = 2.006×10^{-3} and electron mobility = 1.799×10^{-3} cm²V⁻¹s⁻¹ for **P64**). Moreover, **P64** based films showed a proper size of phase separation in the nano-network structure: beneficial for charge transport for improved FF and J_{SC} . The reference polymer (**P66**) based device together with PC₇₁BM gave a comparable PCE of 10.3% with the random terpolymers (Ma et al., 2015).

Tang et al. (2019) reported random terpolymers denoted as **P68** FD21, **P69** FD11, and **P70** FD12 based on monomers having 3,3'-difluoro-2,2'-bithiophene (FTT), fluorinated benzothiadiazole (FBT) and DPP core structures with a 2:1, 1:1, and 1:2 amounts of the FTT -FBT and FTT -DPP segments, respectively. **P67** FD10 and **P71** FD01 (reference polymers) consisting of FBT-FTT and DPP-FTT segments, respectively, were also studied (**Figure 7**). Moreover, the properties of a 1:1 physical blend of **P67** and **P71** were examined. The onset of absorption of the polymers in solid state were found to be 742, 882, 912, 946, and 923 for **P67**, **P68**, **P69**, **P70**, and **P71**, respectively. As presumed, the onset of absorption shifted to longer wavelength with the increase in the DPP content (Zheng et al., 2016). The HOMO energy levels were found to be -5.39, -5.37, -5.35, -5.35, and -5.34 eV, for **P67**, **P68**, **P69**, **P70**, and **P71**, respectively (CV). The HOMO generally lie on the FBT unit and hence an upward shift in

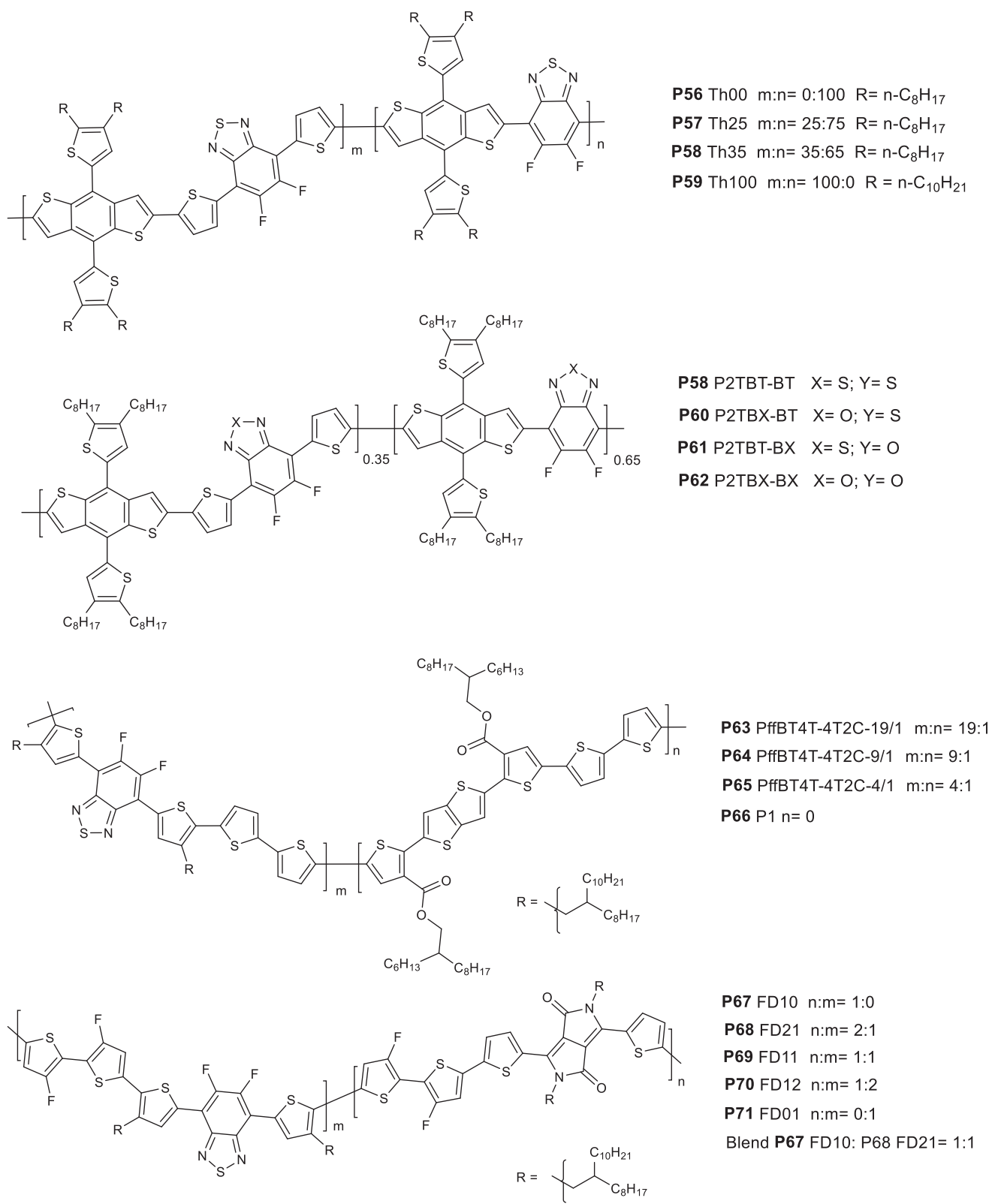
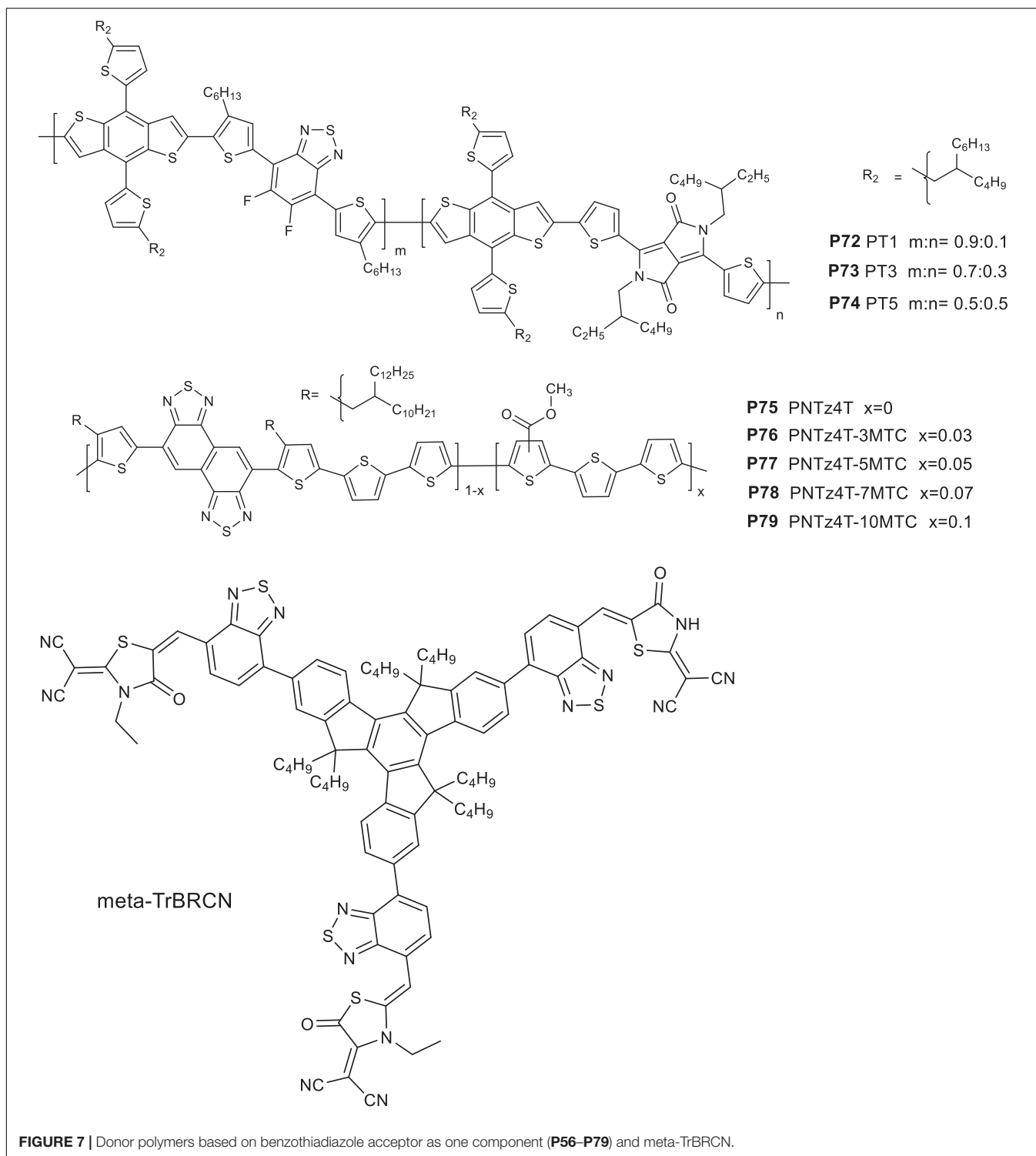


FIGURE 7 | Continued



the values is observed with the decrease in the content of the FBT moiety. The LUMO of **P67**, **P68**, **P69**, **P70**, and **P71** were calculated to be -3.67 , -3.59 , -3.66 , -3.68 , and -3.78 eV, respectively.

PSCs were fabricated using an inverted configuration (ITO/ZnO/polymer: PC₇₁BM/MoO₃/Al), with the active layer

prepared by spin coating from chlorobenzene and DIO. Solar cell devices based on **P67** and **P71** showed a PCE of 6.12 and 3.80%, respectively. The higher performance of the **P67** based device is mainly attributed to the improved V_{OC} and J_{SC} . However, the devices prepared from a 1:2 blend of **P68** and PC₇₁BM gave a PCE as high as 6.41% with the

addition of 2.5% DIO. The high performance was attributed to a balanced hole and electron mobility (2.36×10^{-4} and $2.23 \times 10^{-4} \text{ cm}^2 \text{ V}^{-1} \text{ s}^{-1}$). The devices prepared from **P69** and **P70** gave a maximum PCE of 4.82 and 3.57%, respectively. Interestingly, the PCE of a ternary blend of **P67**, **P68**, and PC₇₁BM in a 0.5:0.5:1.5 (wt/wt ratio respectively) was 7.04% with a corresponding $J_{SC} = 13.79 \text{ mA/cm}^2$, $V_{OC} = 0.77 \text{ V}$ and $FF = 66\%$. The respectable J_{SC} of the ternary blend is attributed to a broader and complimentary optical absorption.

The FBT and DPP based acceptors were also reacted with a BDT based monomer to yield terpolymers namely **P72** PT1, **P73** PT3, and **P74** PT5 with 10, 30, and 50% of a BDT-DPP segment in the backbone, respectively (Xu et al., 2019a; Figure 7). Upon increase in the BDT-DPP segment content, a broad and red shifted absorption spectrum was observed. Moreover, the frontier orbital energy levels, charge transport and morphological compatibility were optimized by changing the feed ratio of the monomeric units in the terpolymer (Xie et al., 2018). Absorption study revealed the main absorption bands appear in the range of 550–850 nm, while the absorption bands shifting to longer wavelength with the increase in the DPP unit. This is consistent with the result observed with terpolymers prepared from FTT, FBT and DPP based monomers (Tang et al., 2019). Hence, **P74** with an equal content of the BDT-DPP and BDT-BT segment in the backbone of the polymer (assuming that the feed ratio is same as to the ratio of monomer fraction installed in the polymer backbone), have the most red shifted absorption peak compared to that of **P72** and **P73**. Two acceptors [meta-TrBRCN (Figure 7) and ITCPTC (Figure 4)] have been used to evaluate the photovoltaic properties of the materials. The main absorption peak of meta-TrBRCN and ITCPTC are close to 500 nm and 750 nm, respectively, which compliments the absorption spectrum of the polymers. The HOMO/LUMO levels were $-4.90/-3.33 \text{ eV}$, $-4.88/-3.35 \text{ eV}$, and $-4.86/-3.35 \text{ eV}$ for the **P72**, **P73**, and **P74**, with a slight shift in the values. Using meta-TrBRCN blended with each of the polymers, the best PCE was 9.61% obtained from **P74** while **P72** and **P73** gave 8.75 and 9.47%, respectively. Looking at the device parameters, the V_{OC} and J_{SC} of the devices fabricated using the three polymers are close to each other while a difference was observed in the FF of the devices. While **P73** and **P74** based devices showed a FF of 74 and 76%, respectively, **P72** based device showed a 71% FF. In addition, **P73** and **P74** based devices showed a smoother morphology compared to **P72** based films (AFM and TEM study) and thus explaining the relatively better performance of both **P73** and **P74** based devices. Moreover, a ternary blend that consist of **P73**, meta-TrBRCN (0.3) and ITCPTC (0.7) were used to fabricate photovoltaic device which gave a $J_{SC} = 20.16 \text{ mA/cm}^2$, $FF = 76.3\%$, and $PCE = 13.63\%$.

The use of random terpolymers to control crystallinity and aggregation of naphtho[1,2-c:5,6-c']bis[1,2,5]thiadiazole based polymers have been explored. Rasool et al. (2019) reported **P75** PNTz4T, **P76** PNTz4T-3MTC, **P77** PNTz4T-5MTC, **P78** PNTz4T-7MTC, and **P79** PNTz4T-10MTC terpolymers

prepared from (2-decyltetradecyl)thiophen-2-yl)naphtho[1,2-c:5,6-c']bis[1,2,5]thiadiazole, 5,5'-bis-(2,2'-bithiophen-2-yl) and methyl thiophene-3-carboxylate (MTC). **P75** is a reference polymer having (2-decyltetradecyl)thiophen-2-yl)naphtho[1,2-c:5,6-c']bis[1,2,5]thiadiazole and 5,5'-bis-(2,2'-bithiophen-2-yl) (Figure 7). The absorption bands of the polymers are at 400–500 nm and 650–750 nm. Among these polymers, **P77** gave a PCE of 9.66% with 0.12 cm^2 cell area, when fabricated at room temperature in a halogen-free solvent (Rasool et al., 2019).

Benzotriazole Ring Based Polymers

Benzotriazole based monomers have been widely used for the synthesis of medium band gap D-A polymers (Price et al., 2011; Gedefaw et al., 2016b).

In a recent study, random terpolymers based on fluorinated benzotriazole, cyano benzotriazole and BDT monomers were reported and properties were compared with a ternary blend of two alternating polymers and PC₇₁BM (Figure 8; Kelly et al., 2018). The random terpolymers are prepared from CNTAZ and FTAZ in 9:1 **P81**, 7:3 **P82**, 1:1 **P83**, 3:7 **P84**, and 1:9 **P85** feed ratios, respectively. **P80** MonoCnTAZ and **P86** FTAZ are the reference polymers. The terpolymers and ternary blends showed similar optical absorption behavior. The photovoltaic properties of the polymers were investigated (ITO/CuSCN/BHJ/Ca/Al). The highest efficiency achieved was 8.25% from **P81** based device. A ternary blend consisting **P80**, **P86** (9:1 ratio) and the acceptor gave a PCE up to 7.92%. The details of the properties are tabulated in Table 7.

Guo et al. (2018) used thiazolothiazole (TTz), fluorinated benzotriazole and a 2D-BDT based monomers to yield random terpolymers with 20% (**P88** PSBTZ-80), 40% (**P89** PSBTZ-60), and 60% (**P90** PSBTZ-40) of the BDT-TTz segment.

A thioalkyl substituted thiophene was attached to the BDT core unit to exploit the advantage of a 2D molecular units (Guo et al., 2018). The reference polymers containing BDT-Tz (**P87** PSBZ) and BDT-TTz (**P91** PSTZ) were also studied (Figure 8). The polymers showed similar optical properties, with an absorption peak and shoulder peak appearing at 545 and 594 nm, respectively. A gradual down ward shift of the HOMO and LUMO energy levels was observed with the increase in the TTz content. The HOMO/LUMO values **P87** and **P91** are $-5.37/-3.44$ and $-5.44/-3.48 \text{ eV}$, respectively while the energy levels of the random terpolymers are between those of the binary polymers.

To probe the photovoltaic properties, a device structure of ITO/ZnO/PFN/polymers: ITIC/MoO₃/Al was used. A device based on a 1:1 blend of **P89** and ITIC processed from toluene gave a PCE of 9.1% due to the relatively higher J_{SC} (16.5 mA/cm^2) and increased to 10.3% with 1% DPE additive. Devices fabricated based on **P87**, **P88**, **P90**, and **P91** yielded a PCE of 8.1, 9.3, 9.3, and 8.5%, respectively. The better performance of **P89** based devices was presumably due to: (i) an improved J_{SC} , (ii) a smoother blend film (**P89**:ITIC) with a smaller rms (1.17 nm) compared to **P87**:ITIC (2.23 nm), **P88**:ITIC (1.80 nm), **P90**:ITIC (1.77 nm), and **P91**:ITIC (1.73 nm), (iii) >95% PL quenching of **P89**:ITIC, and (iv) relatively balanced hole/electron

TABLE 7 | Summary of optical, electrochemical, and photovoltaic properties of polymers (**P80–P94**).

Polymer	λ onset (nm)	HOMO (eV)	LUMO (eV)	J_{SC} (mA/cm ²)	V_{OC} (V)	FF (%)	PCE (%)	Acceptor	References
P80	–	–	–	13.30	0.935	68.9	8.57	PC ₆₁ BM	Kelly et al., 2018
P81	–	–	–	12.62	0.922	68.1	7.92	PC ₆₁ BM	Kelly et al., 2018
P82	–	–	–	12.36	0.904	69.5	7.77	PC ₆₁ BM	Kelly et al., 2018
P83	–	–	–	12.37	0.899	66.7	7.42	PC ₆₁ BM	Kelly et al., 2018
P84	–	–	–	11.98	0.863	68.7	7.11	PC ₆₁ BM	Kelly et al., 2018
P85	–	–	–	11.57	0.834	68.5	6.61	PC ₆₁ BM	Kelly et al., 2018
P86	–	–	–	11.76	0.811	70.7	6.74	PC ₆₁ BM	Kelly et al., 2018
P87	637	–5.37	–3.44	14.7	0.89	61.5	8.1	ITIC	Guo et al., 2018
P88	637	–5.39	–3.45	16.5	0.90	62.4	9.3	ITIC	Guo et al., 2018
P89	637	–5.40	–3.46	18.0	0.91	62.7	10.3	ITIC	Guo et al., 2018
P90	637	–5.41	–3.46	15.7	0.93	63.2	9.3	ITIC	Guo et al., 2018
P91	637	–5.44	–3.48	14.9	0.96	59.1	8.5	ITIC	Guo et al., 2018
P92	650	–5.27	–3.24	6.0	0.85	56	2.9	PC ₆₁ BM	Pang et al., 2019
P93	650	–5.27	–3.23	10.3	0.82	64	5.4	PC ₆₁ BM	Pang et al., 2019
P94	650	–5.26	–3.23	11.1	0.82	69	6.3	PC ₆₁ BM	Pang et al., 2019
P92	–	–	–	11.2	0.87	70	6.8	N2200	Pang et al., 2019
P93	–	–	–	9.4	0.88	60	5.0	N2200	Pang et al., 2019
P94	–	–	–	4.4	0.86	60	2.3	N2200	Pang et al., 2019
P92	–	–	–	14.7	0.91	66	8.8	ITIC	Pang et al., 2019
P93	–	–	–	12.6	0.89	60	6.7	ITIC	Pang et al., 2019
P94	–	–	–	10.6	0.86	60	5.50	ITIC	Pang et al., 2019

mobilities (μ_h/μ_e) ($6.27/3.65 \times 10^{-4}$) (space charge limited current method).

Cao's group investigated the role of alkyl side chain length in terpolymers based on alkylthienyl substituted BDT, difluorinatedbenzotriazole (TAZ) and thienopyrroledione (TPD) monomeres (Pang et al., 2019). The terpolymers are denoted as **P92** PTAZ-TPD10-C10, **P93** PTAZ-TPD10-C8, and **P94** PTAZ-TPD10-C6 with $n\text{-C}_{10}\text{H}_{21}$, $n\text{-C}_8\text{H}_{17}$ and $n\text{-C}_6\text{H}_{13}$ alkyl side chains, respectively, attached to the 2D-BDT based monomer (**Figure 8**). The polymers showed similar optical band gap (1.91 eV). A 30 nm red shift in the solid state absorption was observed due to the high aggregation tendency compared to the solution state. The HOMO and LUMO energy levels of the polymers were calculated to be similar (\sim –5.27 and –3.23 eV), respectively. The photovoltaic properties of the polymers were tested by blending each of the polymers with PC₇₁BM, N2200 (**Figure 8**), ITIC (**Figure 2**) [(ITO/PEDOT:PSS)/active layer/PFN-Br/Al]. Interestingly, the PCE, J_{SC} and FF decreased with shorter alkyl side chains blended with the non-fullerene acceptors (N2200 and ITIC). However, the V_{OC} was not affected by the alkyl chain length. The highest PCE recorded were 6.8 and 8.8% when **P92** was blended with N2200 and ITIC, respectively. The PCE of the devices based on **P94** blended with N2200 and ITIC were 2.3 and 5.5%, respectively. Surprisingly, the opposite trend was observed when PC₇₁BM was used. In this case, the PCE of the devices were 2.9, 5.4, and 6.3% for **P92**, **P93**, and **P94**, respectively. The difference in photovoltaic properties of the polymers with the acceptors is explained by taking morphology into account. For instance, **P94** (shorter alkyl chain) showed a

better miscibility, contracted domains, and favorable vertical phase distribution that encourages charge transport and suppressed recombination.

Benzodithiophenedione (BDD) Ring Based Polymers

The BDD core unit is another acceptor used for the development of terpolymers (**Figure 9**) (**P95–P107**). It is to be noted that D-A alternating polymer based on NTDO and dithienosilole is known to give a moderate performance solar cell (Cui et al., 2011). A D-A polymer consisting of thio alkyl side chain modified NTDO and chlorine-substituted BDT (PBN-Cl) based monomers was reported by Li's group (Wu Y. et al., 2019). The same group have recently investigated the effect of the addition of a BDD monomeric unit as third component to the NTDO and BDT based monomers to yield a series of random terpolymers denoted as **P95** PBN-Cl, **P96** PBN-Cl-B20, **P97** PBN-Cl-B40, **P98** PBN-Cl-B60, **P99** PBN-Cl-B80 and **P100** PBDB-T-2Cl, with 0, 20, 40, 80, and 100% of the BDD-BDT-Cl segment, respectively (**Figure 9**; Yang et al., 2019). For comparison, reference alternating polymers were also studied. A blue shift was noticed with the increase in the content of the BDD-BDT segment in UV-visible spectrum. Hence, the polymer with the lowest band gap in the series (1.8 eV) is **P95** (contain no BDD component). While there is no significant change in the HOMO energy levels, the LUMO, however, showed a successive upward shift as the BDD-BDT segment content increases.

IT-4F (**Figure 9**) was used as an acceptor to investigate the photovoltaic properties of the polymers [(ITO)/PDEOT:PSS/polymer:IT-4F/ZnO/Al]. The device

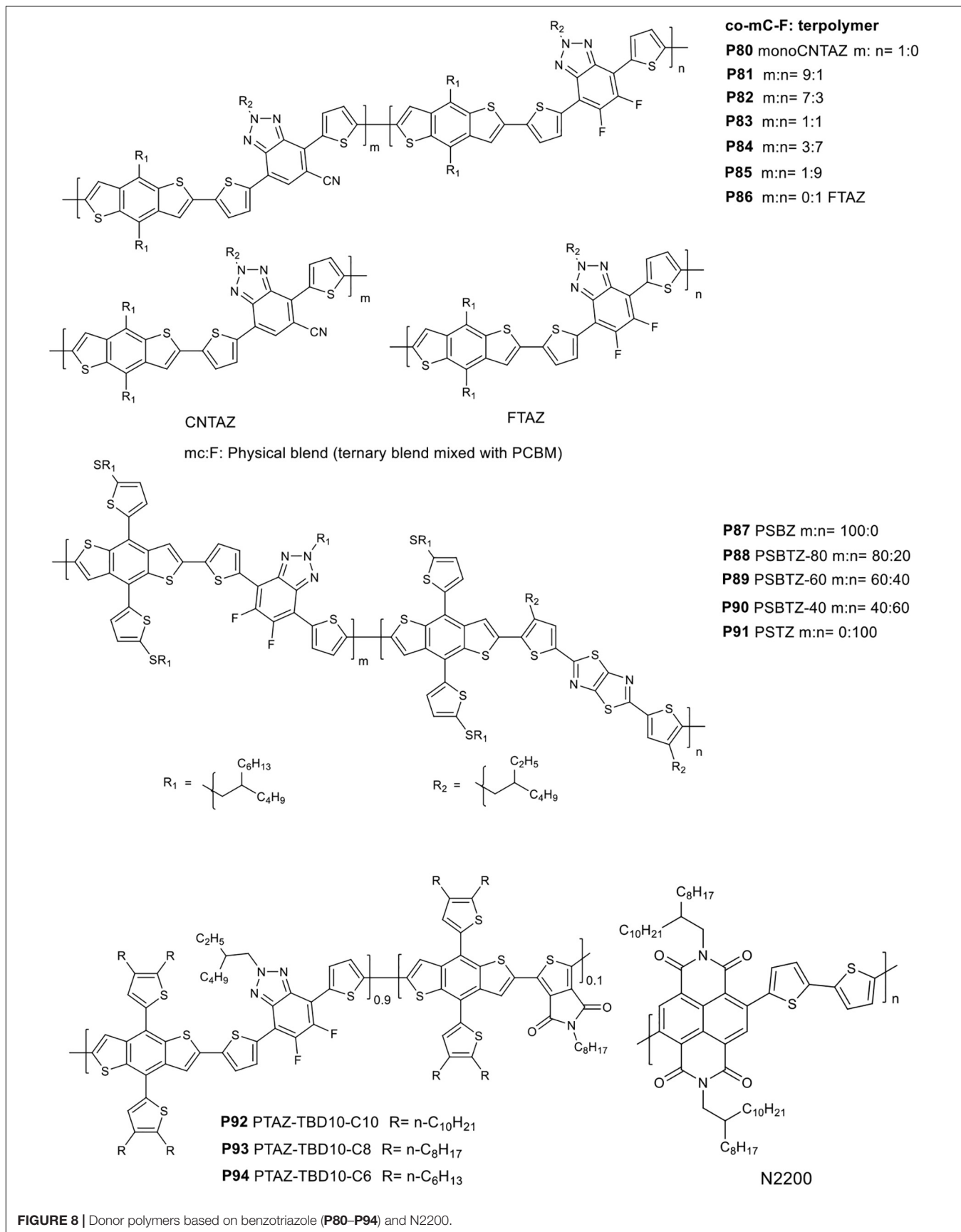
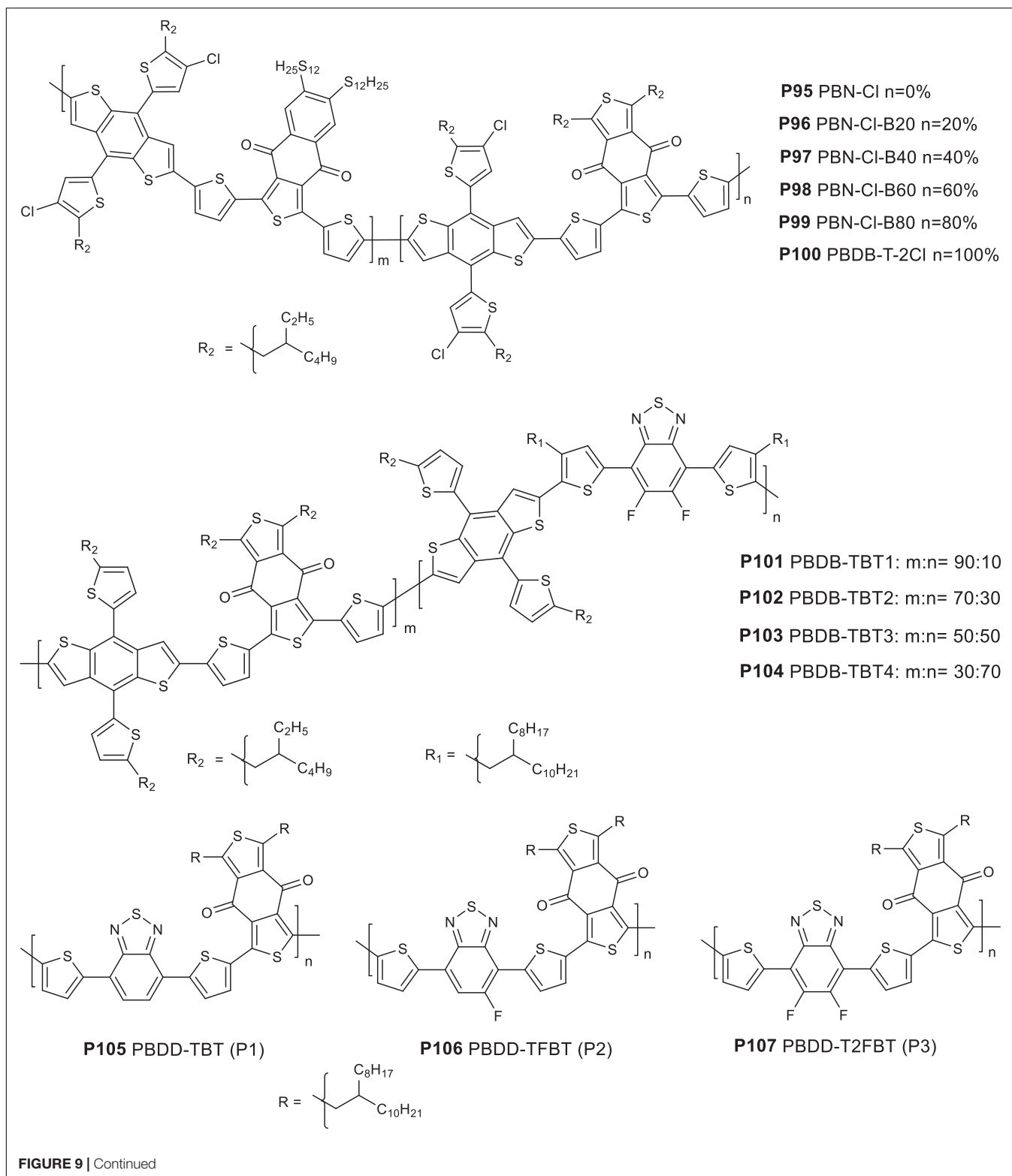


FIGURE 8 | Donor polymers based on benzotriazole (P80–P94) and N2200.



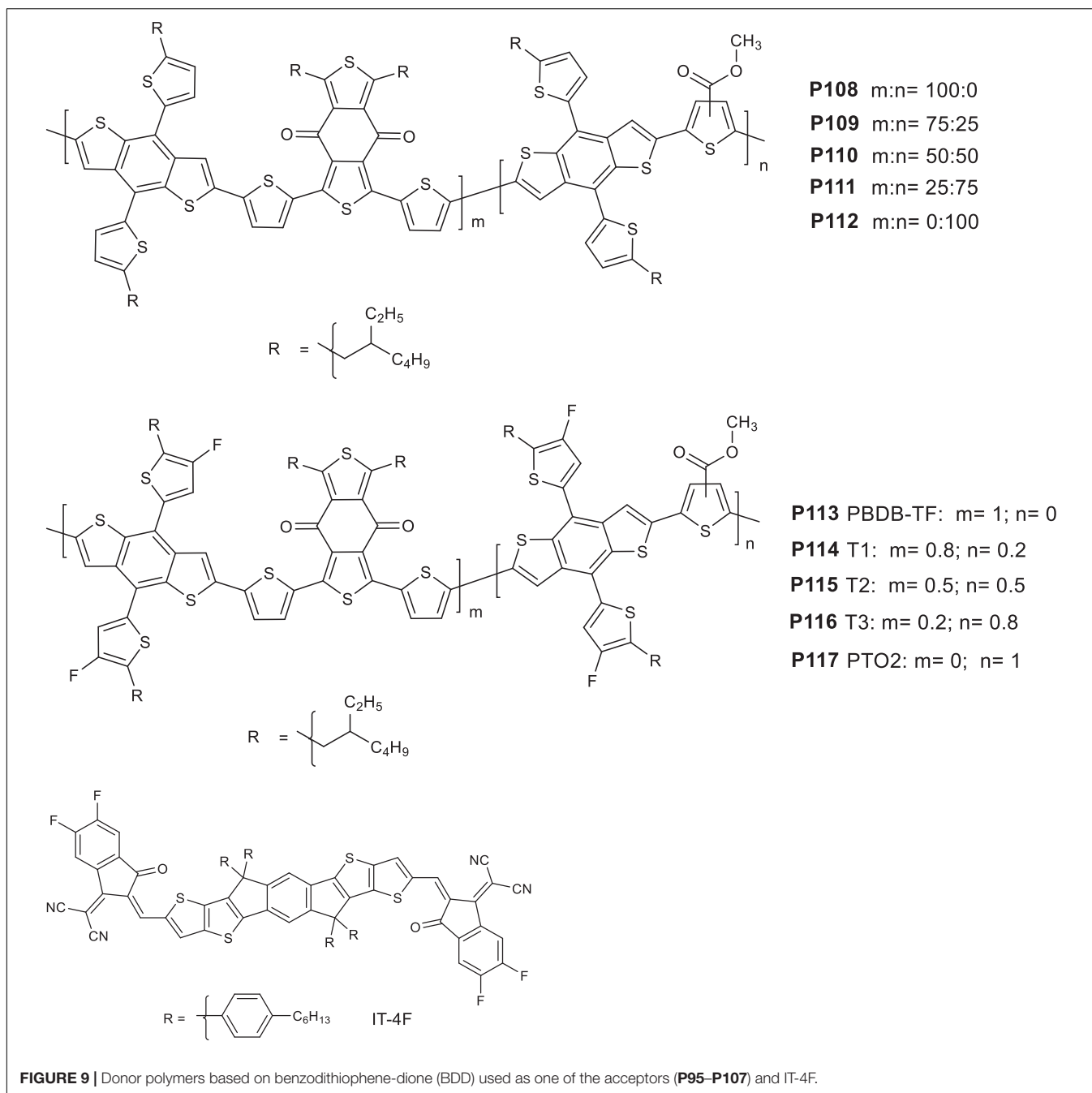


FIGURE 9 | Donor polymers based on benzodithiophene-dione (BDD) used as one of the acceptors (**P95–P107**) and IT-4F.

based on **P95** yielded a 11.21% PCE, $V_{OC} = 0.868$ V, $J_{SC} = 21.01$ mA/cm², and FF = 61.5%. With the introduction of the BDD monomer, the FF showed an improvement reaching to 72.1% for the device prepared based on **P99**. Hence, **P99** based device demonstrated the highest PCE = 14.05%, $J_{SC} = 21.85$ mA/cm² and $V_{OC} = 0.891$ V. Device based on **P100** however showed an outstanding PCE of 14.08% with $V_{OC} = 0.885$ V, a $J_{SC} = 21.41$ mA/cm², and a FF = 74.3%. Even though the overall performances of **P99** and **P100** devices are comparable, both J_{SC} and V_{OC} of the devices based on the terpolymer (**P99**) were higher indicating terpolymerization as a feasible strategy

to fine-tune the photovoltaic properties. Charge transport study showed a balanced hole and electron mobility of the film prepared from a **P99**:IT-4F. Moreover, **P99**:IT-4F film showed a well-developed and more uniform phase separation (TEM), benefiting FF and J_{sc} of the devices.

Wu M. et al. (2019) combined BDD, difluorobenzothiadazole (BT) and BDT based monomers to construct a series of PBDB-TBTn random terpolymers. The amount of the BDT-BT based segment were 10, 30, 50, and 70% in **P101** PBDB-TBT1, **P102** PBDB-TBT2, **P103** PBDB-TBT3, and **P104** PBDB-TBT4, respectively (**Figure 9**). The random terpolymers revealed similar

absorption tendency in both solution and solid-state, with the peaks appearing from 300 nm to 700 nm. The absorption onset of the polymers are in the range of 693 nm to 708 nm. The HOMO and LUMO energy levels (CV measurement) are estimated to be $-5.30/-3.42$, $-5.33/-3.45$, $-5.35/-3.47$, and $-5.36/-3.45$ eV for **P101**, **P102**, **P103**, and **P104**, respectively. Obviously, the HOMO levels showed a gradual down-shift with the increase in the BT based monomer content due its electron-deficiency. The same trend was observed for the LUMO energy levels except the mismatch for **P104**. The photovoltaic performances investigation (ITO/ZnO/polymer:ITIC/MoO₃/Ag) showed a drop with the increase of the BDT-BT content. The highest PCE recorded was 9.09% with a $V_{OC} = 0.86$ V, a $J_{SC} = 16.84$ mA/cm² and FF = 62.85% from **P101** based device. The devices based on **P102**, **P103** and **P104** displayed a PCE of 7.95, 5.93 and 2.09%, respectively. The better performance of **P101** based devices is explained by the high and balanced hole and electron mobility (4.12×10^{-4} cm²V⁻¹s⁻¹ and 4.74×10^{-4} cm²V⁻¹s⁻¹), well-distributed microstructural morphologies and smaller domain sizes (10–20 nm).

Kini et al. (2018), reported regular terpolymers consisting of BT, BDD and thiophene (**Figure 9**). The terpolymers showed broad absorption coverage in the range of 300 and 750 nm. The blue shift in the onset of absorption with the increasing content of the fluorine atom is ascribed to the weakening of conjugation due to the strong electron withdrawing effect of the fluorine atom/s. The HOMO/ LUMO of the **P105** PBDD-TBT, **P106** PBDD-TFBT, and **P107** PBDD-T2FBT was estimated to be $-5.57/-3.89$, $-5.62/-3.92$, and $-5.67/-3.94$,

respectively (CV). The downward shift in the HOMO values with the presence of fluorine atoms is known to have a positive effect for the V_{OC} of the devices. In an inverted device structure (ITO/ZnO/active layer/MoO₃/Ag), a 1:0.8 ratio **P107** and PC₇₁BM based device gave a PCE of 5.97%, $V_{OC} = 0.99$ V, $J_{SC} = 8.96$ mA/cm² and FF = 67.6%. The maximum PCEs obtained from **P105** and **P106** based devices were 1.33 and 1.55%, respectively. The better performance of **P107** based devices is ascribed to the strong interchain interaction, face on polymer orientation and higher crystallinity of the film, which have contributed to a higher hole mobility of the devices (hole mobility of **P107** based devices = 4.92×10^{-3} cm²V⁻¹s⁻¹ compared to the hole mobility of **P105** and **P106** based devices (3.67×10^{-3} cm²V⁻¹s⁻¹ and 1.86×10^{-3} cm²V⁻¹s⁻¹, respectively).

To tune the polymer properties, the BDD, methyl-3-thiophenecarboxylate (3MT) and BDT based monomers were reacted in different mixing ratio to give **P109**, **P110**, and **P111** (random terpolymers) with 25, 50, and 75% of the BDT-BDD segment in the backbone. **P108** and **P112** are alternating polymers with the backbones made of the BDT-3MT and BDT-BDD segments, respectively (**Figure 9**; Hoang et al., 2019). It is to be noted that a BDT-BDD containing polymer combined with ITIC was known to provide a high efficiency in solar cells (Zhao et al., 2016). The absorption peaks of the terpolymers were located between **P108** (539 nm) and **P112** (625 nm), where the peaks shifted to longer wavelength with BDT-BDD segment content increase. Hence, the solid state absorption peak was found to be at 569, 574, and 616 nm,

TABLE 8 | Summary of optical, electrochemical, and photovoltaic properties of polymers (**P95–P117**).

Polymer	λ onset (nm)	HOMO (eV)	LUMO (eV)	J_{SC} (mA/cm ²)	V_{OC} (V)	FF (%)	PCE (%)	Acceptor	References
P95	688.8	-5.55	-3.54	21.01	0.868	61.5	11.21	IT-4F	Yang et al., 2019
P96	685	-5.55	-3.52	21.55	0.856	63.8	11.77	IT-4F	Yang et al., 2019
P97	681.2	-5.55	-3.50	21.89	0.863	69.8	13.18	IT-4F	Yang et al., 2019
P98	677.5	-5.55	-3.48	21.21	0.858	69.9	12.73	IT-4F	Yang et al., 2019
P99	673.8	-5.55	-3.47	21.85	0.891	72.1	14.05	IT-4F	Yang et al., 2019
P100	670.2	-5.55	-3.45	21.41	0.885	74.3	14.08	IT-4F	Yang et al., 2019
P101	693	-5.30	-3.42	16.84	0.86	62.85	9.09	ITIC	Wu M. et al., 2019
P102	696	-5.33	-3.45	15.50	0.88	58.26	7.95	ITIC	Wu M. et al., 2019
P103	698	-5.35	-3.47	11.45	0.91	56.91	5.93	ITIC	Wu M. et al., 2019
P104	708	-5.36	-3.45	4.12	0.90	56.80	2.12	ITIC	Wu M. et al., 2019
P105	740	-5.57	-3.89	2.55	0.86	60.3	1.33	PC ₇₁ BM	Kini et al., 2018
P106	726	-5.62	-3.92	2.96	0.93	57.8	1.55	PC ₇₁ BM	Kini et al., 2018
P107	718	-5.67	-3.94	8.96	0.99	67.6	5.97	PC ₇₁ BM	Kini et al., 2018
P108	625	-5.42	-3.44	15.59	0.97	54.38	8.22	ITIC	Hoang et al., 2019
P109	664	-5.38	-3.51	15.76	0.95	59.76	8.95	ITIC	Hoang et al., 2019
P110	677	-5.37	-3.54	17.18	0.94	63.52	10.26	ITIC	Hoang et al., 2019
P111	681	-5.37	-3.55	17.19	0.90	61.77	9.56	ITIC	Hoang et al., 2019
P112	687	-5.34	-3.54	16.30	0.88	61.48	8.82	ITIC	Hoang et al., 2019
P113	681.2	-5.45	-3.64	20.5	0.863	78	13.8	IT-4F	Cui et al., 2019
P114	677.5	-5.48	-3.63	21.5	0.899	78	15.1	IT-4F	Cui et al., 2019
P115	663.0	-5.51	-3.62	21.3	0.909	75	14.5	IT-4F	Cui et al., 2019
P116	642.4	-5.55	-3.61	21.6	0.920	70	13.9	IT-4F	Cui et al., 2019
P117	623.0	-5.60	-3.57	21.5	0.925	73	14.5	IT-4F	Cui et al., 2019

respectively, for **P109**, **P110**, and **P111**. Similarly, onset of absorption shifted to longer wavelength with the increase in the content of the BDT-BDD segment. The solid state optical band gaps were estimated to be 1.98, 1.87, 1.83, 1.82, and 1.80 eV for **P108**, **P109**, **P110**, **P111**, and **P112**, respectively. The HOMO and LUMO energy levels of the polymers gradually moved to higher-lying and lower-lying positions, respectively, as the content of the BDD unit increases. Hence, **P112** have a HOMO and LUMO of -5.34 and -3.54 compared to -5.42 and -3.44 eV for **P108**. The HOMO and LUMO values of the rest of the polymers were found to lie between that of **P108** and **P112**.

To evaluate the photovoltaic properties of the polymers, a non-fullerene BHJ PSCs were fabricated (ITO/ZnO/polymer:ITIC/MoO₃/Ag). Each of the polymers were blended with ITIC in a 1:1 wt%. Interestingly, the PSCs fabricated from the terpolymers showed an impressive V_{OC} of more than 0.9 V and J_{SC} of more than 15 mA/cm². In detail, the highest V_{OC} was 0.97 V achieved from **P108** devices while the lowest V_{OC} was 0.88 V extracted from **P112** based devices. **P110** (50% of BDT-BDD segment) and **P111** (75% of BDT-BDD segment) based devices gave the highest J_{SC} reaching more than 17.18 mA/cm². Consistently, **P110** gave the highest FF reaching to about 63.52%. The combination of the parameters have offered a 10.26% PCE based on **P110** based devices. The best device efficiency based on **P111** was found to be 9.56% PCE, slightly lower than that of the **P110** based device. The devices prepared based **P108**, **P109**, and **P112** offered a 8.22, 8.95, and 8.82% PCE, respectively. In order to understand the differences in the performance of the polymers in solar cells, the hole and electron mobility of the films were studied. The study showed that a blend of **P110** and ITIC gave a balanced hole and electron mobility with a ratio of 3.37, which have likely contributed toward the higher FF values of the devices. Moreover, a TEM image on **P110**:ITIC blend film showed a more homogeneous and fine domains, that maximizes the charge separation and collection.

The effect of fluorine atom substitution on a BDT donor unit combined with 3MT and BDD based monomers were also studied. In this work, alternating polymers containing either BDD-BDT (**P113** PBDB-TF) or 3MT-BDT (**P117** PTO2) were reported. Additionally, three random terpolymers represented as **P114** T1, **P115** T2, and **P116** T3 with 20, 50, and 80% of 3MT-BDT segments, respectively, are also reported (Figure 9; Cui et al., 2019). With the increase in the content of 3MT-BDT in the backbone, it was possible to finely tune the properties of the resulting polymers. For instance, a blue shift in the optical absorption with higher content of 3MT-BDT was observed. Hence, **P117** (consist of 3MT-BDT) revealed the most blue shifted onset of absorption (623.0 nm) while **P113** (has 0% 3MT-BDT) showed the most red shifted onset of absorption (681.2 nm). The three random terpolymers have an onset of absorption intermediate between the two alternating polymers (**P117** and **P113**). The terpolymers have wider absorptions at the full width at half maximum (FWHM), which is due to the contributions of different segments in the chains. In the electrochemical study, a gradual downward-shift in the HOMO

levels were observed with the increase of the thiophene ester (3MT) content. The opposite trend was observed with the LUMO energy levels. Photovoltaic devices with an inverted structure were fabricated (ITO/ZnO/photoactive layer/MoO₃/Al). An increase in the V_{OC} was observed with the increase of ester group-substituted thiophene content. Moreover, the J_{SC} of all the terpolymer:IT-4F devices are higher (wide FWHM) than that **P113**:IT-4F-based devices. However, a decrease in the PCE going from **P114** to **P116** was mainly due to the decrease in the FF. Among the devices, the highest PCE recorded was 15.1% from a blend of **P114** and IT-4F with corresponding $J_{SC} = 21.5$ mA/cm², $V_{OC} = 0.899$ V, and FF = 78% processed from CB with DIO solvent additive. The devices prepared from **P113**, **P115**, **P116**, and **P117** gave a PCE of 13.8, 14.5, 13.9, and 14.5%, respectively (Table 8). The relatively higher performance of the **P114** based device could arise from the smooth surfaces with small rms values (below 2 nm) which favors charge transport.

SUMMARY AND OUTLOOK

The synthesis of conjugated polymers is an ongoing research for various applications in organic electronics. Recently, the development of terpolymers have gained a wider attention and is being intensively studied. With the synthesis of terpolymers, key properties such as light absorption, energy levels, morphology and charge carrier mobility can be optimized, which have enabled to achieve over 14% PCE in single layer solar cells. Further development of optimized monomers, synthesis of multi chromophore polymers and understanding of structure- property relationships is anticipated to further enhance the PCE of solar cells. One of the key challenges with the synthesis of random terpolymers is the little understanding of the composition along the backbone of the polymer, as the latter will depend on the reaction kinetics of the monomers. For most of the random terpolymers reported to date, the contribution of the different monomers in the polymer backbone is not known for certainty in spite of the known composition of the monomers in the feed of the polymerization reaction.

AUTHOR CONTRIBUTIONS

DG drafted the manuscript. XP and MA edited the manuscript. All authors have contributed to the modification and correction of the manuscript.

ACKNOWLEDGMENTS

We would like to thank the Australian Research Council's Discovery Projects funding scheme (Project DP170102467) for supporting this research. DG thanks the Faculty of Science and Technology (FSTE), The University of the South Pacific (USP) for the financial support.

REFERENCES

- Aernouts, T., Aleksandrov, T., Girotto, C., Genoe, J., and Poortmans, J. (2008). Polymer based organic solar cells using ink-jet printed active layers. *Appl. Phys. Lett.* 92:033306. doi: 10.1063/1.2833185
- Alkan, E., Göker, S., and Toppare, L. (2020). The impact of [1,2,5]chalcogenazolo[3,4-f]-Benzo[1,2,3]Triazole structure on the optoelectronic properties of conjugated polymers. *J. Polym. Sci.* 58, 956–968. doi: 10.1002/pol.20190275
- Almeida, S., Rivera, E., Reyna-González, J., Huerta Angeles, G., Tapia, F., and Aguilar-Martínez, M. (2009). Synthesis and characterization of novel polythiophenes bearing oligo(ethylene glycol) spacers and crown ethers. *Synthetic Metals* 159, 1215–1223. doi: 10.1016/j.synthmet.2009.02.020
- Atlı, G. Ö., Yılmaz, E. A., Aslan, S. T., Udum, Y. A., Toppare, L., and Çırpan, A. (2020). Synthesis and characterization of optical, electrochemical and photovoltaic properties of selenophene bearing benzodithiophene based alternating polymers. *J. Electroanal. Chem.* 862:114014. doi: 10.1016/j.jelechem.2020.114014
- Bang, S.-M., Kang, S., Lee, Y.-S., Lim, B., Heo, H., Lee, J., et al. (2017). A novel random terpolymer for high-efficiency bulk-heterojunction polymer solar cells. *RSC Adv.* 7, 1975–1980. doi: 10.1039/c6ra27518d
- Beimling, P., and Koßmehl, G. (1986). Synthesis of benzo[1,2-b':4,5-b'']dithiophene and its 4,8-Dimethoxy and 4,8-dimethyl derivatives. *Chem. Berichte* 119, 3198–3203. doi: 10.1002/cber.19861191025
- Bolognesi, M., Gedefaw, D., Dang, D., Henriksson, P., Zhuang, W., Tassarolo, M., et al. (2013). 2D π -conjugated benzo[1,2-b':4,5-b'']dithiophene- and quinoxaline-based copolymers for photovoltaic applications. *RSC Adv.* 3, 24543–24552.
- Bolognesi, M., Prosa, M., Tassarolo, M., Donati, G., Toffanin, S., Muccini, M., et al. (2016). Impact of environmentally friendly processing on polymer solar cells: performance, thermal stability and morphological study by imaging techniques. *Solar Energy Mater. Solar Cells* 155, 436–445. doi: 10.1016/j.solmat.2016.06.044
- Bronstein, H., Frost, J. M., Hadipour, A., Kim, Y., Nielsen, C. B., Ashraf, R. S., et al. (2013). Effect of fluorination on the properties of a donor-acceptor copolymer for use in photovoltaic cells and transistors. *Chem. Mater.* 25, 277–285. doi: 10.1021/cm301910t
- Cai, Y., Huo, L., and Sun, Y. (2017). Recent advances in wide-bandgap photovoltaic polymers. *Adv. Mater.* 29:1605437. doi: 10.1002/adma.201605437
- Cao, J., Liao, Q., Du, X., Chen, J., Xiao, Z., Zuo, Q., et al. (2013). A pentacyclic aromatic lactam building block for efficient polymer solar cells. *Energy Environ. Sci.* 6, 3224–3228.
- Cao, J., Zuo, C., Du, B., Qiu, X., and Ding, L. (2015). Hexacyclic lactam building blocks for highly efficient polymer solar cells. *Chem. Commun.* 51, 12122–12125. doi: 10.1039/c5cc04375a
- Chen, H. (2019). Electron-deficient core fused-ring based non-Fullerene acceptor enables over 15% efficiency in single junction organic solar cells. *Sci. China Chem.* 62, 403–404. doi: 10.1007/s11426-019-9431-8
- Chen, H., Guo, Y., Yu, G., Zhao, Y., Zhang, J., Gao, D., et al. (2012). Highly π -extended copolymers with diketopyrrolopyrrole moieties for high-performance field-effect transistors. *Adv. Mater.* 24, 4618–4622. doi: 10.1002/adma.201201318
- Chen, S., Cho, H. J., Lee, J., Yang, Y., Zhang, Z.-G., Li, Y., et al. (2017). Modulating the molecular packing and nanophase blending via a random terpolymerization strategy toward 11% efficiency nonfullerene polymer solar cells. *Adv. Energy Mater.* 7:1701125. doi: 10.1002/aenm.201701125
- Cheng, Y.-J., Yang, S.-H., and Hsu, C.-S. (2009). Synthesis of conjugated polymers for organic solar cell applications. *Chem. Rev.* 109, 5868–5923. doi: 10.1021/cr900182s
- Cho, H.-H., Kim, S., Kim, T., Sree, V. G., Jin, S.-H., Kim, F. S., et al. (2018). Design of cyanovinylene-containing polymer acceptors with large dipole moment change for efficient charge generation in high-performance all-polymer solar cells. *Adv. Energy Mater.* 8:1701436. doi: 10.1002/aenm.201701436
- Choi, H., Ko, S.-J., Kim, T., Morin, P.-O., Walker, B., Lee, B. H., et al. (2015). Small-bandgap polymer solar cells with unprecedented short-circuit current density and high fill factor. *Adv. Mater.* 27, 3318–3324. doi: 10.1002/adma.201501132
- Chu, T.-Y., Lu, J., Beaupré, S., Zhang, Y., Pouliot, J.-R., Wakim, S., et al. (2011). Bulk heterojunction solar cells using Thieno[3,4-c]pyrrole-4,6-dione and Dithieno[3,2-b:2',3'-d]silole copolymer with a power conversion efficiency of 7.3%. *J. Am. Chem. Soc.* 133, 4250–4253. doi: 10.1021/ja200314m
- Colella, S., Melcarne, G., Mazzeo, M., Gigli, G., Grisorio, R., Suranna, G. P., et al. (2011). Synthesis, characterization and photovoltaic properties of random poly(arylene-vinylene)s containing benzothiadiazole. *Polymer* 52, 2740–2746. doi: 10.1016/j.polymer.2011.04.066
- Cui, C., Fan, X., Zhang, M., Zhang, J., Min, J., and Li, Y. A. D. (2011). –A copolymer of dithienosilole and a new acceptor unit of naphtho[2,3-c]thiophene-4,9-dione for efficient polymer solar cells. *Chem. Commun.* 47, 11345–11347.
- Cui, Y., Yao, H., Hong, L., Zhang, T., Xu, Y., Xian, K., et al. (2019). Achieving over 15% efficiency in organic photovoltaic cells via copolymer design. *Adv. Mater.* 31:1808356. doi: 10.1002/adma.201808356
- Deng, Z., Wu, F., Chen, L., and Chen, Y. (2015). Novel photovoltaic donor 1-acceptor-donor 2-acceptor terpolymers with tunable energy levels based on a difluorinated benzothiadiazole acceptor. *RSC Adv.* 5, 12087–12093. doi: 10.1039/c4ra15181j
- Duan, C., Furlan, A., van Franeker, J. J., Willems, R. E. M., Wienk, M. M., and Janssen, R. A. J. (2015). Wide-bandgap benzodithiophene-benzothiadiazole copolymers for highly efficient multijunction polymer solar cells. *Adv. Mater.* 27, 4461–4468. doi: 10.1002/adma.201501626
- Duan, C., Gao, K., van Franeker, J. J., Liu, F., Wienk, M. M., and Janssen, R. A. J. (2016). Toward practical useful polymers for highly efficient solar cells via a random copolymer approach. *J. Am. Chem. Soc.* 138, 10782–10785. doi: 10.1021/jacs.6b06418
- Elsenbaumer, R. L., Jen, K. Y., and Oboodi, R. (1986). Processible and environmentally stable conducting polymers. *Synthetic Metals* 15, 169–174. doi: 10.1016/0379-6779(86)90020-2
- Fan, B., Zhang, D., Li, M., Zhong, W., Zeng, Z., Ying, L., et al. (2019). Achieving over 16% efficiency for single-junction organic solar cells. *Sci. China Chem.* 62, 746–752. doi: 10.1007/s11426-019-9457-5
- Fan, B., Zhang, K., Jiang, X.-F., Ying, L., Huang, F., and Cao, Y. (2017). High-performance nonfullerene polymer solar cells based on imide-functionalized wide-bandgap polymers. *Adv. Mater.* 29:1606396. doi: 10.1002/adma.201606396
- Gao, X., Wu, Y., Tao, Y., and Huang, W. (2020). Conjugated random terpolymer donors towards high-efficiency polymer solar cells. *Chin. J. Chem.* 38, 601–624. doi: 10.1002/cjoc.201900503
- Gedefaw, D., and Andersson, M. R. (2019). “Donor-acceptor polymers for organic photovoltaics,” in *Conjugated Polymers Perspective, Theory, and New Materials*, eds J. R. Reynolds, B. C. Thompson, and T. A. Skotheim (Boca Raton, FL: CRC Press), doi: 10.1201/b22235-8
- Gedefaw, D., Ma, Z., Mulugeta, E., Zhao, Y., Zhang, F., Andersson, M. R., et al. (2016a). An alternating copolymer of fluorene donor and quinoxaline acceptor versus a terpolymer consisting of fluorene, quinoxaline and benzothiadiazole building units: synthesis and characterization. *Polym. Bull.* 73, 1167–1183. doi: 10.1007/s00289-015-1541-y
- Gedefaw, D., Prosa, M., Bolognesi, M., Seri, M., and Andersson, M. R. (2017a). Recent development of quinoxaline based polymers/small molecules for organic photovoltaics. *Adv. Energy Mater.* 7:1700575. doi: 10.1002/aenm.201700575
- Gedefaw, D., Sharma, A., Pan, X., Bjuggren, J. M., Kroon, R., Gregoriou, V. G., et al. (2017b). Optimization of the power conversion efficiency in high bandgap pyridopyridinedithiophene-based conjugated polymers for organic photovoltaics by the random terpolymer approach. *Eur. Polym. J.* 91, 92–99. doi: 10.1016/j.eurpolymj.2017.03.044
- Gedefaw, D., Tassarolo, M., Bolognesi, M., Prosa, M., Kroon, R., Zhuang, W., et al. (2016b). Synthesis and characterization of benzodithiophene and benzotriazole-based polymers for photovoltaic applications. *Beilstein J. Organ. Chem.* 12, 1629–1637. doi: 10.3762/bjoc.12.160
- Gedefaw, D., Tassarolo, M., Zhuang, W., Kroon, R., Wang, E., Bolognesi, M., et al. (2014). Conjugated polymers based on benzodithiophene and fluorinated quinoxaline for bulk heterojunction solar cells: thiophene versus thieno[3,2-b]thiophene as π -conjugated spacers. *Polym. Chem.* 5, 2083–2093.

- Gedefaw, D., Zhou, Y., Hellström, S., Lindgren, L., Andersson, L. M., Zhang, F., et al. (2009). Alternating copolymers of fluorene and donor-acceptor-donor segments designed for miscibility in bulk heterojunction photovoltaics. *J. Mater. Chem.* 19, 5359–5363. doi: 10.1039/b817111h
- Glenis, S., Horowitz, G., Tourillon, G., and Garnier, F. (1984). Electrochemically grown polythiophene and poly(3-methylthiophene) organic photovoltaic cells. *Thin Solid Films* 111, 93–103. doi: 10.1016/0040-6090(84)90478-4
- Granström, M., Petritsch, K., Arias, A. C., Lux, A., Andersson, M. R., and Friend, R. H. (1998). Laminated fabrication of polymeric photovoltaic diodes. *Nature* 395, 257–260. doi: 10.1038/26183
- Guo, X., Fan, Q., Cui, C., Zhang, Z., and Zhang, M. (2018). Wide bandgap random terpolymers for high efficiency halogen-free solvent processed polymer solar cells. *Wuli Huaxue Xuebao* 34, 1279–1285.
- Halls, J. J. M., Walsh, C. A., Greenham, N. C., Marseglia, E. A., Friend, R. H., Moratti, S. C., et al. (1995). Efficient photodiodes from interpenetrating polymer networks. *Nature* 376, 498–500. doi: 10.1038/376498a0
- Havinga, E. E., ten Hoeve, W., and Wynberg, H. (1992). A new class of small band gap organic polymer conductors. *Polym. Bull.* 29, 119–126. doi: 10.1007/bf00558045
- Heintges, G. H. L., Bolduc, A., Meskers, S. C. J., and Janssen, R. A. J. (2020). Relation between the electronic properties of regioregular donor-acceptor terpolymers and their binary copolymers. *J. Phys. Chem. C* 124, 3503–3516. doi: 10.1021/acs.jpcc.9b11562
- Hendriks, K. H., Heintges, G. H. L., Gevaerts, V. S., Wienk, M. M., and Janssen, R. A. J. (2013). High-molecular-weight regular alternating diketopyrrolopyrrole-based terpolymers for efficient organic solar cells. *Angew. Chem. Int. Edition* 52, 8341–8344. doi: 10.1002/anie.201302319
- Hendriks, K. H., Heintges, G. H. L., Wienk, M. M., and Janssen, R. A. J. (2014). Comparing random and regular diketopyrrolopyrrole-bithiophene-thienopyrrolo-dione terpolymers for organic photovoltaics. *J. Mater. Chem. A* 2, 17899–17905. doi: 10.1039/c4ta04118f
- Heo, H., Kim, H., Lee, D., Jang, S., Ban, L., Lim, B., et al. (2016). Regioregular D1-A-D2-A terpolymer with controlled thieno[3,4-b]thiophene orientation for high-efficiency polymer solar cells processed with nonhalogenated solvents. *Macromolecules* 49, 3328–3335. doi: 10.1021/acs.macromol.6b00269
- Heo, H., Kim, H., Nam, G., Lee, D., and Lee, Y. (2018). Multi-donor random terpolymers based on benzodithiophene and dithienosilole segments with different monomer compositions for high-performance polymer solar cells. *Macromol. Res.* 26, 238–245. doi: 10.1007/s13233-018-6030-3
- Heuvel, R., Colberts, F. J. M., Li, J., Wienk, M. M., and Janssen, R. A. J. (2018). The effect of side-chain substitution on the aggregation and photovoltaic performance of diketopyrrolopyrrole-alt-dicarboxylic ester bithiophene polymers. *J. Mater. Chem. A* 6, 20904–20915. doi: 10.1039/c8ta05238g
- Hoang, M. H., Park, G. E., Choi, S., Park, C. G., Park, S. H., Nguyen, T. V., et al. (2019). High-efficiency non-fullerene polymer solar cell fabricated by a simple process using new conjugated terpolymers. *J. Mater. Chem. C* 7, 111–118. doi: 10.1039/c8tc05035j
- Hoth, C. N., Choulis, S. A., Schilinsky, P., and Brabec, C. J. (2007). High photovoltaic performance of inkjet printed polymer: fullerene blends. *Adv. Mater.* 19, 3973–3978. doi: 10.1002/adma.200700911
- Hou, J., Park, M.-H., Zhang, S., Yao, Y., Chen, L.-M., Li, J.-H., et al. (2008). Bandgap and molecular energy level control of conjugated polymer photovoltaic materials based on benzo[1,2-b:4,5-b']dithiophene. *Macromolecules* 41, 6012–6018. doi: 10.1021/ma800820r
- Huo, L., Liu, T., Sun, X., Cai, Y., Heeger, A. J., and Sun, Y. (2015). Single-junction organic solar cells based on a novel wide-bandgap polymer with efficiency of 9.7%. *Adv. Mater.* 27, 2938–2944. doi: 10.1002/adma.201500647
- Huo, L., Xue, X., Liu, T., Xiong, W., Qi, F., Fan, B., et al. (2018). Subtle side-chain engineering of random terpolymers for high-performance organic solar cells. *Chem. Mater.* 30, 3294–3300. doi: 10.1021/acs.chemmater.8b00510
- Ie, Y., Huang, J., Uetani, Y., Karakawa, M., and Aso, Y. (2012). Synthesis, properties, and photovoltaic performances of donor-acceptor copolymers having dioxocycloalkene-annelated thiophenes as acceptor monomer units. *Macromolecules* 45, 4564–4571. doi: 10.1021/ma300742r
- Jenkins, A. D., Kratochvil, P., Stepto, R. F. T., and Suter, U. W. (1996). Glossary of basic terms in polymer science. *Pure Appl. Chem.* 68, 2287–2311.
- Jiang, T., Yang, J., Tao, Y., Fan, C., Xue, L., Zhang, Z., et al. (2016). Random terpolymer with a cost-effective monomer and comparable efficiency to PTB7-Th for bulk-heterojunction polymer solar cells. *Polym. Chem.* 7, 926–932. doi: 10.1039/c5py01771h
- Kang, T. E., Cho, H.-H., Kim, H. J., Lee, W., Kang, H., and Kim, B. J. (2013). Importance of optimal composition in random terpolymer-based polymer solar cells. *Macromolecules* 46, 6806–6813. doi: 10.1021/ma401274r
- Kawashima, K., Tamai, Y., Ohkita, H., Osaka, I., and Takimiya, K. (2015). High-efficiency polymer solar cells with small photon energy loss. *Nat. Commun.* 6:10085.
- Kelly, M. A., Zhang, Q., Peng, Z., Noman, V., Zhu, C., Ade, H., et al. (2018). The finale of a trilogy: comparing terpolymers and ternary blends with structurally similar backbones for use in organic bulk heterojunction solar cells. *J. Mater. Chem. A* 6, 19190–19200. doi: 10.1039/c8ta05132a
- Keshtov, M. L., Kuklin, S. A., Konstantinov, I. O., Ostapov, I. E., Makhaeva, E. E., Nikolaev, A. Y., et al. (2019). Random D1-A1-D1-A2 terpolymers based on diketopyrrolopyrrole and benzothiadiazolequinoxaline (BTQx) derivatives for high-performance polymer solar cells. *New J. Chem.* 43, 5325–5334. doi: 10.1039/c8nj05905e
- Khlyabich, P. P., Burkhart, B., Ng, C. F., and Thompson, B. C. (2011). Efficient solar cells from semi-random P3HT analogues incorporating diketopyrrolopyrrole. *Macromolecules* 44, 5079–5084. doi: 10.1021/ma2009386
- Kim, A., Lee, J. H., Kim, H. J., Choi, S., Kim, Y. U., Park, C. G., et al. (2018). New conjugated regular terpolymers based on diketopyrrolopyrrole-benzodithiophene and their application to thin film transistors and polymer solar cells. *Synthetic Metals* 236, 36–43. doi: 10.1016/j.synthmet.2018.01.002
- Kim, S. W., Kim, H., Lee, J.-W., Lee, C., Lim, B., Lee, J., et al. (2019). Synergistic effects of terpolymer regioregularity on the performance of all-polymer solar cells. *Macromolecules* 52, 738–746. doi: 10.1021/acs.macromol.8b02337
- Kini, G. P., Choi, J. Y., Jeon, S. J., Suh, I. S., and Moon, D. K. (2018). Controlling the interchain packing and photovoltaic properties via fluorine substitution in terpolymers based on benzo[1,2-c:4,5-c']dithiophene-4,8-dione and benzothiadiazole units. *Polymer* 148, 330–338. doi: 10.1016/j.polymer.2018.06.038
- Kitamura, C., Tanaka, S., and Yamashita, Y. (1996). Design of narrow-bandgap polymers. syntheses and properties of monomers and polymers containing aromatic-donor and o-quinoid-acceptor units. *Chem. Mater.* 8, 570–578. doi: 10.1021/cm950467m
- Ko, E. Y., Park, G. E., Lee, D. H., Um, H. A., Shin, J., Cho, M. J., et al. (2015). Enhanced performance of polymer solar cells comprising diketopyrrolopyrrole-based regular terpolymer bearing two different π -extended donor units. *ACS Appl. Mater. Interf.* 7, 28303–28310. doi: 10.1021/acsami.5b08510
- Kroon, R., Diaz de Zerio Mendaza, A., Himmelberger, S., Bergqvist, J., Bäcke, O., Faria, G. C., et al. (2014). A new tetracyclic lactam building block for thick, broad-bandgap photovoltaics. *J. Am. Chem. Soc.* 136, 11578–11581. doi: 10.1021/ja5051692
- Kroon, R., Melianas, A., Zhuang, W., Bergqvist, J., Diaz de Zerio Mendaza, A., Steckler, T. T., et al. (2015). Comparison of selenophene and thienothiophene incorporation into pentacyclic lactam-based conjugated polymers for organic solar cells. *Polym. Chem.* 6, 7402–7409. doi: 10.1039/c5py01245g
- Lee, D., Hubijar, E., Kalaw, G. J. D., and Ferraris, J. P. (2012). Enhanced and tunable open-circuit voltage using dialkylthio benzo[1,2-b:4,5-b']dithiophene in polymer solar cells. *Chem. Mater.* 24, 2534–2540. doi: 10.1021/cm3011056
- Li, K., Hu, Z., Zeng, Z., Huang, Z., Zhong, W., Ying, L., et al. (2018). Improved performance of non-fullerene polymer solar cells using wide-bandgap random terpolymers. *Organ. Electron.* 57, 317–322. doi: 10.1016/j.orgel.2018.03.005
- Li, N., Baran, D., Spyropoulos, G. D., Zhang, H., Berny, S., Turbiez, M., et al. (2014). Environmentally printing efficient organic tandem solar cells with high fill factors: a guideline towards 20% power conversion efficiency. *Adv. Energy Mater.* 4:1400084. doi: 10.1002/aenm.201400084
- Li, S., Ye, L., Zhao, W., Yan, H., Yang, B., Liu, D., et al. (2018). Wide band gap polymer with a deep highest occupied molecular orbital level enables 14.2% efficiency in polymer solar cells. *J. Am. Chem. Soc.* 140, 7159–7167. doi: 10.1021/jacs.8b02695

- Li, Z., Lu, J., Tse, S.-C., Zhou, J., Du, X., Tao, Y., et al. (2011). Synthesis and applications of difluorobenzothiadiazole based conjugated polymers for organic photovoltaics. *J. Mater. Chem.* 21, 3226–3233.
- Liang, Y., Feng, D., Wu, Y., Tsai, S.-T., Li, G., Ray, C., et al. (2009a). Highly efficient solar cell polymers developed via fine-tuning of structural and electronic properties. *J. Am. Chem. Soc.* 131, 7792–7799. doi: 10.1021/ja901545q
- Liang, Y., Wu, Y., Feng, D., Tsai, S.-T., Son, H.-J., Li, G., et al. (2009b). Development of new semiconducting polymers for high performance solar cells. *J. Am. Chem. Soc.* 131, 56–57.
- Lindgren, L. J., Zhang, F., Andersson, M., Barrau, S., Hellström, S., Mammo, W., et al. (2009). Synthesis, characterization, and devices of a series of alternating copolymers for solar cells. *Chem. Mater.* 21, 3491–3502. doi: 10.1021/cm802949g
- Liu, Q., Jiang, Y., Jin, K., Qin, J., Xu, J., Li, W., et al. (2020). 18% Efficiency organic solar cells. *Sci. Bull.* 65, 272–275.
- Liu, X., Deng, W., Wang, J., Zhang, R., Zhang, S., Galuska, L., et al. (2019). Energy level modulation of donor–acceptor alternating random conjugated copolymers for achieving high-performance polymer solar cells. *J. Mater. Chem. C* 7, 15335–15343. doi: 10.1039/c9tc05601g
- Liu, Z., Huang, Z., Chen, Y., Xu, T., Yu, H., Guo, X., et al. (2020). Efficient polymer solar cells based on new random copolymers with porphyrin-incorporated side chains. *Macromol. Chem. Phys.* 221:1900446. doi: 10.1002/macp.201900446
- Luo, H., Liu, Z., and Zhang, D. (2018). Conjugated D–A terpolymers for organic field-effect transistors and solar cells. *Polym. J.* 50, 21–31. doi: 10.1038/pj.2017.53
- Luo, Z., Ma, R., Liu, T., Yu, J., Xiao, Y., Sun, R., et al. (2020). Fine-tuning energy levels via asymmetric end groups enables polymer solar cells with efficiencies over 17%. *Joule* 4, 1236–1247. doi: 10.1016/j.joule.2020.03.023
- Ma, W., Yang, G., Jiang, K., Carpenter, J. H., Wu, Y., Meng, X., et al. (2015). Influence of processing parameters and molecular weight on the morphology and properties of high-performance PffBT4T-2OD:PC71BM organic solar cells. *Adv. Energy Mater.* 5:1501400. doi: 10.1002/aenm.201501400
- Meng, L., Zhang, Y., Wan, X., Li, C., Zhang, X., Wang, Y., et al. (2018). Organic and solution-processed tandem solar cells with 17.3% efficiency. *Science* 361, 1094–1098.
- Pan, X., Xiong, W., Liu, T., Sun, X., Huo, L., Wei, D., et al. (2017). Influence of 2,2-bithiophene and thieno[3,2-b] thiophene units on the photovoltaic performance of benzodithiophene-based wide-bandgap polymers. *J. Mater. Chem. C* 5, 4471–4479. doi: 10.1039/c7tc00720e
- Pang, S., Zhang, R., Duan, C., Zhang, S., Gu, X., Liu, X., et al. (2019). Alkyl chain length effects of polymer donors on the morphology and device performance of polymer solar cells with different acceptors. *Adv. Energy Mater.* 9:1901740. doi: 10.1002/aenm.201901740
- Paulsen, B. D., Speros, J. C., Clafin, M. S., Hillmyer, M. A., and Frisbie, C. D. (2014). Tuning of HOMO energy levels and open circuit voltages in solar cells based on statistical copolymers prepared by ADMET polymerization. *Polym. Chem.* 5, 6287–6294. doi: 10.1039/c4py00832d
- Price, S. C., Stuart, A. C., Yang, L., Zhou, H., and You, W. (2011). Fluorine substituted conjugated polymer of medium band gap yields 7% efficiency in polymer-fullerene solar cells. *J. Am. Chem. Soc.* 133, 4625–4631. doi: 10.1021/ja1112595
- Qian, D., Ye, L., Zhang, M., Liang, Y., Li, L., Huang, Y., et al. (2012). Design, application, and morphology study of a new photovoltaic polymer with strong aggregation in solution state. *Macromolecules* 45, 9611–9617. doi: 10.1021/ma301900h
- Qing, L., Zhong, A., Chen, W., Cao, Y., and Chen, J. (2020). Largely improved bulk-heterojunction morphology in organic solar cells based on a conjugated terpolymer donor via a ternary strategy. *Polymer* 186:122050. doi: 10.1016/j.polymer.2019.122050
- Rasool, S., Vu, D. V., Song, C. E., Lee, H. K., Lee, S. K., Lee, J.-C., et al. (2019). Room temperature processed highly efficient large-area polymer solar cells achieved with molecular engineering of copolymers. *Adv. Energy Mater.* 9:1900168. doi: 10.1002/aenm.201900168
- Salim, M. B., Nekovei, R., and Jayakumar, R. (2020). Organic tandem solar cells with 18.6% efficiency. *Solar Energy* 198, 160–166. doi: 10.1016/j.solener.2020.01.042
- SambathKumar, B., Shyam Vinod Kumar, P., Deepakrao, F. S., Kumar Iyer, S. S., Subramanian, V., Datt, R., et al. (2016). Two donor–one acceptor random terpolymer comprised of diketopyrrolopyrrole quaterthiophene with various donor π -linkers for organic photovoltaic application. *J. Phys. Chem. C* 120, 26609–26619. doi: 10.1021/acs.jpcc.6b07479
- Scott, A. J., Gabriel, V. A., Dubé, M. A., and Penlidis, A. (2019). Making the most of parameter estimation: terpolymerization troubleshooting tips. *Processes* 7:444. doi: 10.3390/pr7070444
- Seri, M., Gedefaw, D., Prosa, M., Tassarolo, M., Bolognesi, M., Muccini, M., et al. (2017). A new quinoxaline and isoindigo based polymer as donor material for solar cells: Role of ecofriendly processing solvents on the device efficiency and stability. *J. Polym. Sci. Part A Polym. Chem.* 55, 234–242. doi: 10.1002/pola.28361
- Shin, I., Ahn, H. J., Yun, J. H., Jo, J. W., Park, S., Joe, S.-Y., et al. (2018). High-performance and uniform 1 cm² polymer solar cells with D1-A-D2-A-type random terpolymers. *Adv. Energy Mater.* 8:1701405. doi: 10.1002/aenm.201701405
- Song, S., Keum, S., Lee, J.-H., Lee, J., Kim, S., Park, S. S., et al. (2018). Photovoltaic polymers based on difluoroquinoxaline units with deep HOMO levels. *J. Polym. Sci. Part A Polym. Chem.* 56, 1489–1497. doi: 10.1002/pola.29014
- Stuart, A. C., Tumbleston, J. R., Zhou, H., Li, W., Liu, S., Ade, H., et al. (2013). Fluorine substituents reduce charge recombination and drive structure and morphology development in polymer solar cells. *J. Am. Chem. Soc.* 135, 1806–1815. doi: 10.1021/ja309289u
- Sumaiya, S., Kardel, K., and Shahat, A. E. (2017). “Organic solar cell by inkjet printing – an overview,” in *2017 IEEE SmartWorld, Ubiquitous Intelligence & Computing, Advanced & Trusted Computed, Scalable Computing & Communications, Cloud & Big Data Computing, Internet of People and Smart City Innovation (SmartWorld/SCALCOM/UIC/ATC/CBDCOM/IOP/SCI)*, (San Francisco, CA: IEEE), 1–8.
- Tang, C. W. (1986). Two–layer organic photovoltaic cell. *Appl. Phys. Lett.* 48, 183–185. doi: 10.1063/1.96937
- Tang, F., Wu, K., Duan, K., Deng, Y., Zhao, B., and Tan, S. (2019). Improved photovoltaic performance of D-A1-D-A2 terpolymer via synergetic effects of copolymerization and blending. *Dyes Pigments* 160, 79–85. doi: 10.1016/j.dyepig.2018.07.041
- Tassarolo, M., Gedefaw, D., Bolognesi, M., Liscio, F., Henriksson, P., Zhuang, W., et al. (2014). Structural tuning of quinoxaline-benzodithiophene copolymers via alkyl side chain manipulation: synthesis, characterization and photovoltaic properties. *J. Mater. Chem. A* 2, 11162–11170. doi: 10.1039/c4ta01479k
- Wang, J., Wang, S., Duan, C., Colberts, F. J. M., Mai, J., Liu, X., et al. (2017). Conjugated polymers based on difluorobenzoxadiazole toward practical application of polymer solar cells. *Adv. Energy Mater.* 7:1702033. doi: 10.1002/aenm.201702033
- Wang, N., Chen, Z., Wei, W., and Jiang, Z. (2013). Fluorinated benzothiadiazole-based conjugated polymers for high-performance polymer solar cells without any processing additives or post-treatments. *J. Am. Chem. Soc.* 135, 17060–17068. doi: 10.1021/ja409881g
- Wang, T., Sun, R., Shi, M., Pan, F., Hu, Z., Huang, F., et al. (2020). Solution-processed polymer solar cells with over 17% efficiency enabled by an iridium complexation approach. *Adv. Energy Mater.* 10:2000590. doi: 10.1002/aenm.202000590
- Wang, X., Dou, K., Shahid, B., Liu, Z., Li, Y., Sun, M., et al. (2019). Terpolymer strategy toward high-efficiency polymer solar cells: integrating symmetric benzodithiophene and asymmetrical thieno[2,3-f]benzofuran segments. *Chem. Mater.* 31, 6163–6173. doi: 10.1021/acs.chemmater.9b01957
- Wu, M., Shi, L., Hu, Y., Chen, L., Hu, T., Zhang, Y., et al. (2019). Additive-free non-fullerene organic solar cells with random copolymers as donors over 9% power conversion efficiency. *Chin. Chem. Lett.* 30, 1161–1167. doi: 10.1016/j.ccl.2019.04.029
- Wu, Y., Yang, H., Zou, Y., Dong, Y., Yuan, J., Cui, C., et al. (2019). A new dialkylthio-substituted naphtho[2,3-c]thiophene-4,9-dione based polymer donor for high-performance polymer solar cells. *Energy Environ. Sci.* 12, 675–683. doi: 10.1039/c8ee03608j
- Xie, Q., Liao, X., Chen, L., Zhang, M., Gao, K., Huang, B., et al. (2019). Random copolymerization realized high efficient polymer solar cells with a record

- fill factor near 80%. *Nano Energy* 61, 228–235. doi: 10.1016/j.nanoen.2019.04.048
- Xie, R., Li, Z., Zhong, W., Ying, L., Hu, Q., Liu, F., et al. (2018). Overcoming the morphological and efficiency limit in all-polymer solar cells by designing conjugated random copolymers containing a naphtho[1,2-c:5,6-c']bis([1,2,5]thiadiazole) moiety. *J. Mater. Chem. A* 6, 23295–23300. doi: 10.1039/c8ta09356c
- Xu, X., Bi, Z., Ma, W., Zhang, G., Yan, H., Li, Y., et al. (2019a). Stable large area organic solar cells realized by using random terpolymers donors combined with a ternary blend. *J. Mater. Chem. A* 7, 14199–14208. doi: 10.1039/c9ta03188j
- Xu, X., Feng, K., Bi, Z., Ma, W., Zhang, G., and Peng, Q. (2019b). Single-junction polymer solar cells with 16.35% efficiency enabled by a platinum(II) complexation strategy. *Adv. Mater.* 31:1901872. doi: 10.1002/adma.201901872
- Yang, H., Wu, Y., Dong, Y., Cui, C., and Li, Y. (2019). Random polymer donor for high-performance polymer solar cells with efficiency over 14%. *ACS Appl. Mater. Interfaces* 11, 40339–40346. doi: 10.1021/acsami.9b14133
- Yang, Y., Zhang, Z.-G., Bin, H., Chen, S., Gao, L., Xue, L., et al. (2016). Side-chain isomerization on an n-type organic semiconductor ITIC acceptor makes 11.77% high efficiency polymer solar cells. *J. Am. Chem. Soc.* 138, 15011–15018. doi: 10.1021/jacs.6b09110
- Yohannes, T., Zhang, F., Svensson, M., Hummelen, J. C., Andersson, M. R., and Inganäs, O. (2004). Polyfluorene copolymer based bulk heterojunction solar cells. *Thin Solid Films* 449, 152–157. doi: 10.1016/s0040-6090(03)01348-8
- Yu, G., Gao, J., Hummelen, J. C., Wudl, F., and Heeger, A. J. (1995). Polymer photovoltaic cells: enhanced efficiencies via a network of internal donor-acceptor heterojunctions. *Science* 270, 1789–1791. doi: 10.1126/science.270.5243.1789
- Zhang, F., Jespersen, K. G., Björström, C., Svensson, M., Andersson, M. R., Sundström, V., et al. (2006). Influence of solvent mixing on the morphology and performance of solar cells based on polyfluorene copolymer/fullerene blends. *Adv. Funct. Mater.* 16, 667–674. doi: 10.1002/adfm.200500339
- Zhang, H., Liu, Y., Sun, Y., Li, M., Kan, B., Ke, X., et al. (2017). Developing high-performance small molecule organic solar cells via a large planar structure and an electron-withdrawing central unit. *Chem. Commun.* 53, 451–454. doi: 10.1039/c6cc07927j
- Zhang, H., Yao, H., Hou, J., Zhu, J., Zhang, J., Li, W., et al. (2018). Over 14% efficiency in organic solar cells enabled by chlorinated nonfullerene small-molecule acceptors. *Adv. Mater.* 30:1800613. doi: 10.1002/adma.201800613
- Zhang, Y., Shao, Y., Wei, Z., Zhang, L., Hu, Y., Chen, L., et al. (2020). “Double-acceptor-type” random conjugated terpolymer donors for additive-free non-fullerene organic solar cells. *ACS Appl. Mater. Interf.* 12, 20741–20749. doi: 10.1021/acsami.0c02862
- Zhang, Z.-G., Qi, B., Jin, Z., Chi, D., Qi, Z., Li, Y., et al. (2014). Perylene diimides: a thickness-insensitive cathode interlayer for high performance polymer solar cells. *Energy Environ. Sci.* 7, 1966–1973.
- Zhao, W., Qian, D., Zhang, S., Li, S., Inganäs, O., Gao, F., et al. (2016). Fullerene-free polymer solar cells with over 11% efficiency and excellent thermal stability. *Adv. Mater.* 28, 4734–4739. doi: 10.1002/adma.201600281
- Zheng, Z., Zhang, S., Zhang, J., Qin, Y., Li, W., Yu, R., et al. (2016). Over 11% efficiency in tandem polymer solar cells featured by a low-band-gap polymer with fine-tuned properties. *Adv. Mater.* 28, 5133–5138. doi: 10.1002/adma.201600373
- Zhou, Y., Gedefaw, D. A., Hellström, S., Krättschmer, I., Zhang, F., Mammo, W., et al. (2010). Black polymers in bulk-heterojunction solar cells. *IEEE J. Select. Top. Quant. Electron.* 16, 1565–1572.
- Zou, Y., Najari, A., Berrouard, P., Beaupré, S., Réda Aïch, B., Tao, Y., et al. (2010). Thieno[3,4-c]pyrrole-4,6-dione-based copolymer for efficient solar cells. *J. Am. Chem. Soc.* 132, 5330–5331.

Conflict of Interest: The authors declare that the research was conducted in the absence of any commercial or financial relationships that could be construed as a potential conflict of interest.

Copyright © 2020 Gedefaw, Pan and Andersson. This is an open-access article distributed under the terms of the Creative Commons Attribution License (CC BY). The use, distribution or reproduction in other forums is permitted, provided the original author(s) and the copyright owner(s) are credited and that the original publication in this journal is cited, in accordance with accepted academic practice. No use, distribution or reproduction is permitted which does not comply with these terms.